



# Durham E-Theses

---

## *Duality and resonances*

Yagoobi, Kamal Seyed

### How to cite:

---

Yagoobi, Kamal Seyed (1973) *Duality and resonances*, Durham theses, Durham University. Available at Durham E-Theses Online: <http://etheses.dur.ac.uk/9948/>

### Use policy

---

The full-text may be used and/or reproduced, and given to third parties in any format or medium, without prior permission or charge, for personal research or study, educational, or not-for-profit purposes provided that:

- a full bibliographic reference is made to the original source
- a [link](#) is made to the metadata record in Durham E-Theses
- the full-text is not changed in any way

The full-text must not be sold in any format or medium without the formal permission of the copyright holders.

Please consult the [full Durham E-Theses policy](#) for further details.

**DUALITY / AND RESONANCES**

by

**Kamal Seyed Yagoobi**

**A thesis presented for the degree of Master of Science  
of the University of Durham**

**September 1973**

**Mathematics Department,  
South Road,  
University of Durham,  
England.**



## PREFACE

The work presented in this thesis was carried out in the Department of Mathematics, University of Durham, under the supervision of Professor E.J. Squires. The author expresses his highest appreciation and sincere gratitude to Professor Squires for continuous guidance, encouragement and help.

Special thanks are also due to his friends, Mr Vlossopolos and Mr Webber, from whom he benefited in many interesting discussions during the past year.

## CONTENTS

Preface	ii
Contents	iii
Abstract	iv
CHAPTER 1 : A General Discussion On Resonances And Particle Classification Scheme.	1
CHAPTER 2 : $A_1$ And The Deck Effect.	25
CHAPTER 3 : Duality	34
CHAPTER 4 : Further Investigations And Conclusion	44
References	
Figure Captions	
Tables	
Figures	

ABSTRACT

The main idea of the following pages is to review the  $A_1$  particle. They set out to explain the problem, to show the attempts done in this field and to compare the different interpretations of different authors. In order to do this we use resonances and duality as our tools of investigation.

In chapter one, we give a general discussion on resonances. We show what we mean by a resonance, what the characteristics of resonances may be, and the ways by which resonances are determined. Some mis-leading terminologies and interpretations which occur in this area are also discussed. In the second part, an explanation of  $SU(2)$ ,  $SU(3)$  and quark models has been done. There, the concept of exotic states and their different types are shown.

In chapter two, a sketch of the  $A_1$  particle, since the time it was discovered till the recent time when different types of models have been given in order to resolve or, at least, to clarify and explain the mystery of the  $\pi^p$  enhancement is drawn. Also the  $A_1$ 's future and a simple test, which invokes data to remove the  $A_1$  ambiguity are given.

In chapter three, the idea of duality has been discussed. How duality has altered the concept of resonances, what the conflict with the earlier interference model is, the Veneziano model and finally the effect of duality on the  $A_1$  problem are discussed.

In chapter four, we extend the discussion of chapter three. The excellent discussion by E.L. Berger (1971) is

given here. His suggested model may make the situation of the  $A_1$  clear. His discussion encourages people to believe that the  $A_1$  might be a kinematical effect. Finally, we conclude by giving a brief review of the present status of the  $A_1$  enhancement.

## CHAPTER 1

### A general discussion on resonances and particle classification schemes

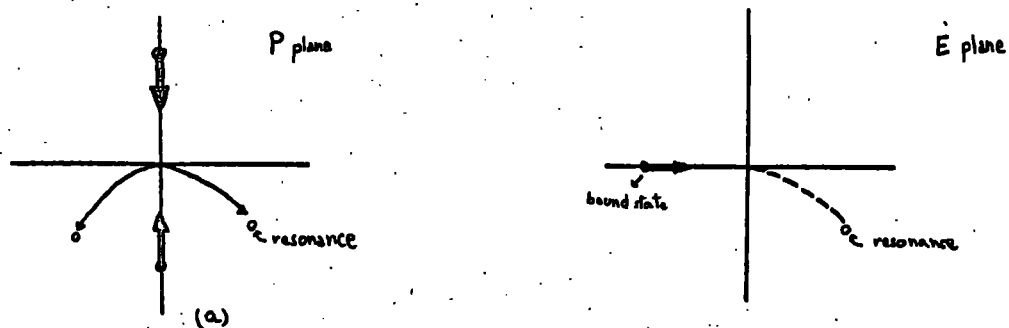
#### PART ONE

### A general discussion on resonances

#### 1.1- INTRODUCTION

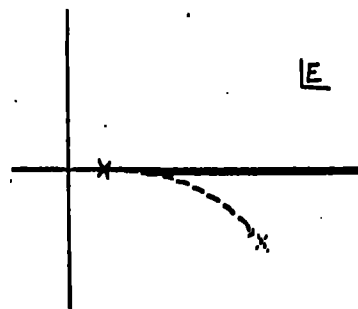
What is a resonance? To answer let us begin with the idea of a 'bound state'. These states exist for example in potential scattering theory where they occur as poles in the scattering amplitude. These poles lie on the positive energy axis below the physical threshold. In relativistic scattering theory one can have poles that arise through 'forces' (i.e. are bound states) and also possibly some that are simply added to the S matrix. We do not distinguish between these and regard them all as 'particles'.

In potential scattering it is possible to weaken the potential so that the bound state pole moves above the physical threshold. It then becomes an unstable particle and can decay into its constituents. This decay is characterized by an average life-time  $\tau$ .



(a) Transition of a bound state into a resonance. (b) Corresponding motion in the E plane.

As long as  $\tau$  is reasonably large we can observe these unstable particles in essentially the same way as we observe stable particles, for example by tracks in a bubble chamber. Clearly whether a particle is stable or unstable depends on its mass and the mass of other particles (and also on various conservation rules). It is not a fundamental property of the particle, so it is natural to regard stable and unstable particles as being objects of the same kind, (they are usually referred to simply as 'particles'). The pole corresponding to an unstable particle is below real axis\* (because of unitarity). A physical understanding of why a resonance pole must occur on an unphysical sheet, below the real axis, results from considering the Fourier transform of the resonant amplitude as a function of time. As a resonant system is going to decay after a time  $t$ , the time dependence  $\exp(-iE_r t)$  implies that  $\text{Im } E_r$  must be negative.



Particles which decay by weak interactions, for example,



have life-time of the order of  $10^{-9}$  sec. and so such particles can be seen. However, it turns out that particles that decay by electromagnetic interactions, e.g.,



or strong interactions, e.g.,



\* These poles, i.e. the resonance poles, should be nearby poles. That is, they should not be located far from the real axis, as otherwise, they are not detectable.

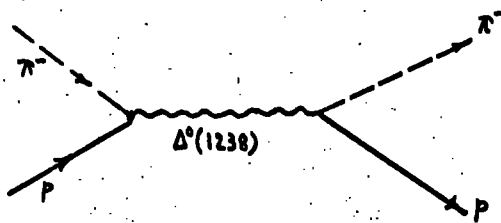
have lifetime  $\tau$  about  $10^{-16}$  sec. and  $10^{-23}$  sec. respectively, so that they do not travel far enough to be observed as particles. In fact, strongly decaying particles do not travel outside the range of nuclear force ( $\sim 10^{-13}$  cm). The question then arises as to how such particles must be observed. It is clear that we cannot observe them directly, since they are off the real energy axis where we cannot do experiments. However a pole near the real axis is likely to give rise to a peak in the cross-section (we discuss the form of this in section 1.2), so we expect to see evidence for resonance by looking for bumps in amplitudes as functions of energy variables.

Two questions may arise now:

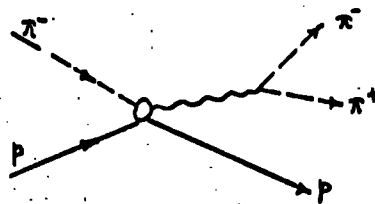
- i) Are there poles which are not resonances of the above type ?
- ii) If we see a bump, does it belong to a 'pole' ?

Later in this chapter, we are going to come back to the second question in a way. We would like to add here, in connection with these questions, that there are systems for which the situation is not so simple, that is, some resonances do not correspond to poles of  $S$ , and on the other hand, some poles of  $S$  do not correspond to resonances (Taylor, 1972; page 241), (Calucci & Ghirardi, 1968).

Generally, there are two types of processes in which resonances appear. These are formation and production mechanisms. The figures below clarify the concept of the mechanisms :



Formation



Production

Perhaps it is worth mentioning that no mesonic resonances, unlike the production mechanisms, have been seen experimentally in formation processes so far. This is not too surprising since the only processes which are experimentally possible and which have the correct quantum numbers are  $\bar{B}B$  experiments. If the baryon and antibaryon annihilate to form mesons then the available energy is such that one is likely to be in a region where resonance overlaps strongly so that individual states will not be seen.

## 1.2- RESONANCE DETERMINATIONS

Now that we know what a resonance is, let us see the ways of its determination. In this section we will be studying the Dalitz plot, the Argand diagram and the Breit-Wigner formula.

### 1.2.1- Dalitz Plot.

A particularly useful technique in the study of resonances in production experiments, involving three particles in the final state, is the Dalitz plot. In this plot each event is represented by a point. The Dalitz diagram is frequently made in terms of the effective mass\* square of particle pairs. The alternative is to

---

\* The effective mass,  $m_{\text{eff}}$ , of a group of  $i$  particles is defined as:

$$\begin{aligned} m_{\text{eff}}^2(1,2,\dots,i) &= (p_1 + p_2 + \dots + p_i)^2 \\ &= \left( \sum_{n=1}^i E_n \right)^2 - \left( \sum_{n=1}^i \mathbf{p}_n \right)^2 \end{aligned}$$

where  $p_j$  is the four momentum of  $j_{\text{th}}$  particle.

plot number of events against the effective mass of three final particles. One can show (Martin-Spearman, 1970; page 163) that phase space alone predicts a uniform distribution of points within the boundary of an effective mass plot. Supposing that two (2 and 3) of the three final particles (1,2,3) form a resonant state of mass  $M^*$ , then we expect a concentration of events to lie along the straight line  $s_{23} = M^{*2}$  across the effective mass plot.

A modification of the plot is often useful for a large number of final particles. For instance, in the reaction  $ab \rightarrow 1234$ , one plots  $m_{\text{eff}}^{2(1,2)}$  against  $m_{\text{eff}}^{2(3,4)}$ . In figures 1 and 2, two Dalitz plots one for a three particle final state and the other for the case of four particle final state have been represented.

### 1.2.2- The Breit-Wigner Formula\*.

As we saw before, the most familiar type of unphysical sheet pole lies at a complex point, say  $P$ , in the  $s$ -plane, slightly below the physical region, e.g. at a position  $s_p = s_R - i\gamma$ , where  $\gamma$  is a small positive and real quantity. To consider the physical effect of this pole, let us expand

$$g(s) \equiv (s-s_p) T_j(s)$$

in a power series about the point  $s=s_p$

$$g(s) \approx g(s_p) + (s-s_p) g'(s_p) + \dots \quad (1.1)$$

The remainder of this expansion, that is the dot terms are sometimes called the 'background' of the resonance. The series (1.1) is convergent in a circle that includes part of the physical region as shown in figure 5.

As  $\gamma$  is a small quantity, we may assume that for  $s$  (physical)

---

\* Another approach to derive the Breit-Wigner formula is given by Hughes(1972).

near  $s_R$  we can write

$$g(s) \approx g(s_p)$$

which in turn leads us to the famous Breit-Wigner resonance formula

$$T_j(s) \underset{s \text{ near } s_R}{\approx} -g(s_p)/(s_R - s - i\Gamma)$$

from which one easily identifies the conventional parameter  $\Gamma$  as

$$\Gamma = \mathcal{V}/(s_R)^{\frac{1}{2}}.$$

Unitarity (for partial wave amplitudes)

$$\text{Im } T_j(s) = \frac{1}{2} T_j(s)^2$$

demands that the residue function must be of the form of

$$g(s_p) \sim -2\Gamma (s_R)^{\frac{1}{2}}.$$

And time reversal makes the residue function to be real.

As was mentioned before, one of the experimental indications of the existence of the resonances is the peaks in cross sections as a function of energy. However, the Breit-Wigner formula is a means by which we can extrapolate down the physical region (i.e. the peak of the cross section from the data) to unphysical sheet pole (i.e. the theoretical resonance) in order to calculate the parameters of the resonances. The extrapolation can be and sometimes is improved by keeping more terms in the expansion (1.1). Note that the location parameters of a resonance, i.e.  $s_R$  and  $\Gamma$ , do not depend on the particular mechanism in which the resonance is observed. It is the residue of the pole and the background which differ, not the position.

### 1.2.3- Argand Diagram.

We know that one can expand the scattering amplitude  $F(s, \cos \theta)$  of any process of the form  $ab \rightarrow cd$  in a series of partial wave amplitudes which are functions of only one of the variables. For example for the scattering of spinless particles one can write

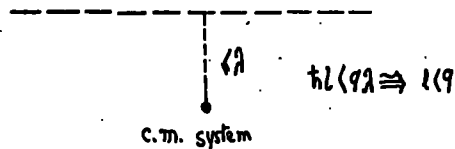
$$F(s, \cos \theta) = \sum_{j=0}^{\infty} (2j+1) T_j(s) P_j(\cos \theta) \quad (1.2)$$

where  $\theta$  and  $j$  are the center of mass scattering angle and the total angular momentum, respectively. Evidently this series cannot con-

verge for all  $s$  and  $\theta$ , for  $P_j$  with  $j$  a positive integer (including zero) is an entire function of  $\cos\theta (\sim t)$ , since the partial wave is independent of  $\theta$ , that is, it is holomorphic, free of singularities for finite  $t$ , therefore  $F(s, \cos\theta)$  can have no singularities in  $\cos\theta (\sim t)$ . But the series will break down at the nearest ( $t$ ) singularity. The domain of convergence of a Legendre polynomial expansion such as this one (eq. 1.2) is the interior of the largest ellipse, the Lehmann ellipse. This can be drawn in the  $\cos\theta$  plane with  $\pm 1$  as foci and with the semi-major axis  $\cos\theta$  such that it does not enclose any singular points of the amplitude. This is a well known result in complex variable theory (see, for example, Titchmarsh, 1939).

The expansion (1.2) is certainly appropriate for those partial waves for which there occur resonance states in the energy range considered, and for which the partial wave amplitudes are therefore rapidly varying. In such an expansion it is necessary to restrict the number of partial waves to those for which the partial wave analysis give an acceptable fit to the data. A 'quasi reason' for the truncating of partial waves is to suppose  $\lambda$  be the range of the force of the longest range contributing to the scattering ( $\sim \hbar$ , since the longest range interaction comes from

the exchange of one pion). Considering the diagram below, if the particles are to interact, they



must come within a distance  $\lambda$  of each other. Therefore if the distance between the particles at the point of nearest approach is less than  $\lambda$  then the angular momentum of the two particle system cannot exceed  $\lambda q (\sim \hbar q)$ . So the  $j$ th partial wave will only contribute to the scat-

---

\* In particular, the series is convergent for all physical  $\theta$ 's.

tering when the center of mass three-momentum is greater than or equal to a value of about  $\hbar l$  ( $l \ll q$ ).

The Argand diagram provides an elegant way of describing the energy dependence of a partial wave amplitude  $T_j$ . The diagram is plotted in a two coordinate system with the imaginary part of the partial wave amplitude against the real part of it. Let us take the background terms of the scattering amplitude as well as the resonant term into consideration before an explanation of the Argand diagram. By background scattering we mean the non resonant scattering in the resonating partial waves plus the other partial waves. In this energy region the scattering amplitude  $F(s, \cos\theta)$  takes the form

$$F(s, \cos\theta) = \sum_i \frac{B_i}{s - M_i^2} P_{j_i}(\cos\theta) + B(s, \cos\theta)$$

where  $M_i$  is the mass value for resonance  $i$ ,  $j_i$  its angular momentum and  $B(s, \cos\theta)$  is the background amplitude.

For simplicity and as the elastic scattering is of particular interest, let us consider this special case. Thus, following Dalitz and Moorhouse (1970),

$$S_j = B_j + i \frac{\Gamma_j}{E_R - E} \exp(2i\chi_j),$$

where,

$$B_j = \sum_\lambda (\Lambda_{j\lambda})^2 \exp(2i\chi_\lambda),$$

$$E_R = E_0 - \frac{1}{2}i\Gamma$$

and  $\chi_j$  and  $\chi_\lambda$  are given in the reference, but we need not worry about them. Here we have used  $S_j$  instead of  $F^{el}(s, \cos\theta)$  of (1.2). Converting S matrix to T, which is defined as

$$T_j = \frac{S_j - 1}{2i}$$

we may write the amplitude in the form (Michael, 1966)

$$T_j = -\frac{1}{2}i(B_j - 1) + \chi_{R_j} \exp(2i\chi_j) \exp(i\sigma) \sin\sigma$$

where  $\eta_{R_j} = \frac{\Gamma_j}{\Gamma} \ll 1$  and  $\sigma$  is the resonance phase defined by

$$\tan \sigma = \Gamma/2(E_0 - E).$$

The background term may be written as

$$-\frac{1}{2}i(B_j - 1) = \eta_B \sin \delta_B \exp(i\delta_B) \quad (1.3)$$

with  $\eta_B \ll 1$ .

For phenomenological analysis, it is usual to adopt the form

$$T_j = -\frac{1}{2}i(\eta_j \exp(2i\delta_j) - 1).$$

The equation above shows that in an Argand diagram for  $\eta_R = 1$ , i.e. for elastic scattering,  $2T_j$  lies on a circle with the center along the imaginary axis with coordinates  $(0, \frac{1}{2})$  and radius  $\frac{1}{2}$ . For inelastic processes,  $\eta_{R_j}$  becomes less than one and, therefore,  $2T_j$  moves in from the circle.

We shall be concerned with the case where the background scattering is energy independent. That is to say,  $\eta_B$  and  $\delta_B$  are constants. Now with the above information and the equations in hand, we have represented the parameters as well as the amplitudes in an Argand plot in figure three. As another example, in fig. 4, we have given four typical resonance configurations (Donnachie, 1970).

Let us see now if there are other mechanisms which generate circles in the Argand diagram, and if any, how one can interpret them. Schmid(1968) has shown that the partial wave projection of a crossed channel Regge pole contribution can result in partial wave amplitudes which generate circles in the Argand diagram as energy increases. These circles are named 'Schmid loops'. It is natural (and perhaps straightforward) to think of these loops as representative of resonances. But the situation is not so simple. In fact there have been various objections, (Collins et al, 1968; Alessandrini et al, 1968; and many others (for the other references see Schmid (1969)), to this interpretation and it has been proposed to consider these circles as something different from resonance circles. Schmid (1969) has removed the objections. He has shown that the Regge pole exchange is not 'another mechanism' as Collins et al would say, that produces loops; rather, it is the usual mechanism (the 'force') that produces the

resonances. This is what duality states. We refer the reader to chapter three for a detailed discussion on duality. Briefly, duality expresses the relation between two descriptions of the hadronic scattering amplitude : at low energy, the description by direct channel (i.e. s-channel) resonance is useful, and on the other hand, the exchange of Regge poles (i.e. t-channel) is more convenient at high energies. So, in some average sense, the s-channel resonances are the t-channel Regge exchanges and vice versa.

Another crucial point in identifying Schmid loops with resonances is the fact that these loops do not contain poles 'directly', corresponding to resonances in the second sheet. We can get rid of this simply by noting that duality is some sort of approximation and we should not expect to have all the detailed information. Let us give a rough example :

Consider the process  $\pi^+ \pi^- \rightarrow \pi^+ \pi^-$  where u-channel is exotic (no resonances) and t-channel is equivalent to s-channel. The Veneziano model\* in this case is (Schmid, 1970)

$$A = -c \Gamma(1-\alpha_s) \Gamma(1-\alpha_t) / \Gamma(1-\alpha_s-\alpha_t)$$

where  $\alpha_s = \frac{1}{2} + s$ . We easily see that  $\Gamma(1-\alpha_s)$  has poles at  $\alpha_s = 1, 2, 3, \dots$

Let us perform a dispersion relation at fixed t. Because of the poles, the dispersion integral simplifies and becomes a sum of pole terms

$$\begin{aligned} A(s, t) &= \frac{1}{\pi} \int_0^{\infty} ds' \frac{D_s A(s', t)}{s' - s} \\ &= \sum_i \frac{1}{M_i^2 - s} P_{j_i}(z) \end{aligned}$$

where  $D_s$  is the discontinuity ( $\equiv \frac{1}{2i} (A(s'+i\epsilon, t) - A(s'-i\epsilon, t))$ ) along the s-channel and  $z = \cos\theta_{ct}$ . Now, when the dispersion integral in s diverges, one needs subtraction constants, e.g.  $a_0 + a_1 s$ . However, these

---

\* For a description of the Veneziano model see, however, the third chapter.

constants in  $s$  are functions of  $t$ , and they will contain the pole (here, the  $\rho$  pole) :

$$a_0 + a_1 s = 2P_1(z_t)/(M_\rho^2 - t) .$$

This is what we meant by 'indirect'.

In the final part of this section we would like to see how one can get the resonance parameters from an Argand diagram. Many criteria have been suggested for this purpose :

- 1) Maximum Modulus. If the background is negligible, then the resonance mass is correlated with the maximum of  $|T_j(s)|$ .
- 2) Top of the Loop. In the case of elastic scattering (1) reduces to the fact that the top of the loop gives the resonance mass.
- 3) Maximum Velocity. Provided  $dB/ds$  is very small, then velocity  $|dT/ds|$  in the Argand plot is maximum at resonance energy position ( $s=s_R$ ).

Phillips and Ringland (1970) tested these criteria in a Veneziano model for  $\pi\pi \rightarrow \pi\omega$  where the resonance parameters were known exactly. Their conclusions were

- 1) For the most prominent resonances all criteria give good results.
- 2) The velocity criterion is consistently good, until resonances overlap strongly.
- 3) The modulus criterion is not very reliable.
- 4) The  $\text{Im } T$  criterion works well in many cases, although the usual justification - real residues - is not true in general.

### 1.3- SOME POSSIBLE QUESTIONS

Here we briefly discuss the possible questions that may arise from the previous notes.

- 1) S matrix poles. We saw that resonances are the poles of S matrix. Now, is it not possible that the S matrix might have several different kinds of poles, of which only one category is appropriately associated with particles? To answer, Chew(1966) introduces the idea of 'channel invariant\*'. He says that all simple poles in individual

---

\* The channel invariant is the square of the total energy in the c.m. system of the channel.

channel invariants are of a simple basic type.

ii) Threshold Enhancements. A state close to threshold (like an s-wave bound state) causes a large cross-section which is called a threshold enhancement. An example of this situation is shown in Fig. 6. The term 'threshold enhancement' is often used with the implication that one is not dealing with a 'true' particle. If, however, extrapolation around the branchpoint clearly indicates the existence of a pole, this situation, therefore, must correspond to a particle state. The essential point is that, in principle, data of sufficient accuracy will always answer this question. We would like to add that most of the threshold enhancements have turned out to be reflections of nearby poles. And when poles are absent, threshold effects are usually too weak to be observable.

iii) Peaks and Resonances. Is a simple peak associated with several different sets of quantum numbers a resonance? We know that the quantum numbers of the particle are the quantum numbers of the coupled channels\*. If the S matrix possesses an exact symmetry, rotational invariance say, then there exist multiplets of equivalent channels and therefore multiplets of equivalent poles. One, however, can say that the multiplets are different particles of exactly the same mass and other quantum numbers (each multiplet to be considered as one particle). We see that such a convention has no confusion when there exists an exact, and completely understood, symmetry. Controversy arises when approximate or accidental degeneracies are available. It seems better to say that each different simple pole corresponds to a different particle. But occasionally one hears the

---

\* Coupled or communicating channel is in the same sense that if sufficient energy were available, the particle could decay into this channel.

terms 'particle' or 'resonance' employed in referring to a 'bump' that detailed analysis has shown to be associated with two or more different poles of the S-matrix lying near each other. This is a misleading terminology that creates confusion. Unless an exact symmetry is involved, each simple pole of the S matrix is in principle separately identifiable and may be assigned a definite set of conserved quantum numbers.

\*\*\*\*\*/

## P A R T T W O

### Particle classification scheme

Je pense qu'il y aurait intérêt à introduire dans l'étude des phénomènes physiques les considérations sur la symétrie familière aux cristallographes.

Pierre Curie

#### 1.4- INTRODUCTION

The discovery of such a wealth of apparently 'elementary' particles stimulated new activity in the search for a pattern amongst them, as a first step towards the understanding of their nature. Since 1956, when Sakata<sup>\*</sup> proposed his model, great emphasis has been laid on the symmetries of the various particles, and a certain amount of order has now emerged out of what appeared previously to be a rather chaotic situation. The particles are classified in certain sets, and

---

\* The introduction of intrinsic symmetries is of course much older and originates with the idea of isotopic spin.

as a result, some of their basic properties are no longer independent.

In this part, we propose to study  $SU(2)$  and  $SU(3)$ . We shall see how particles can be classified. At the end, quarks and quark model will be discussed.

### 1.5- GROUP $SU(2)$

Let  $\Psi_j (j=1,2,\dots,N)$  be an  $N$ -component field. An infinitesimal rotation in isospin space produces the transformation  $\Psi \rightarrow \mathcal{U} \Psi$  where the matrix  $\mathcal{U}$ , with unitarity, can be written as

$$\mathcal{U} = e^{i\phi} U$$

where  $\phi$  is the (real) phase and  $U$  is the modulus of  $\mathcal{U}$ .

We shall restrict the matrix  $U$  to be unitary as well as unimodular. That is

$$\mathcal{U} \mathcal{U}^\dagger = \mathcal{U}^\dagger \mathcal{U} = 1, \quad \det U = 1.$$

Now, instead of talking about rotations in isospin space, one can work with these matrices,  $U$ .

The set of these unitary, unimodular matrices forms the group  $SU(2)$ . From the experience of rotation in Euclidean space, let us write  $U$  as

$$U = \exp\left(\frac{i}{2} \sum_{j=1}^3 \tau_j \theta_j\right)$$

where  $\theta_j$  are three real parameters, the angles of rotation about the axis in isospin space. The three  $N$  by  $N$  matrices  $\tau_j$  are hermitian and traceless and are called the generators of the group.

Let us suppose  $N=2$ . An infinitesimal rotation in isospin space of

$$q = \begin{pmatrix} p \\ n \end{pmatrix} \quad \text{with} \quad \begin{matrix} I_3 & B & S \\ \frac{1}{2} & 1 & 0 \\ -\frac{1}{2} & 1 & 0 \end{matrix}$$

is

$$q \longrightarrow Uq = \exp\left(\frac{i}{2} \sum_{j=1}^3 \tau_j \delta\theta_j\right) \begin{pmatrix} P \\ n \end{pmatrix}.$$

Here  $\tau_j$  are 2x2 matrices which can be taken as Pauli matrices. But following Hendry (1965) we shall use the generators  $A_\nu^\mu$ , the linear combination of Pauli matrices, defined by

$$(A_\nu^\mu)_{ij} = (\delta_{\mu i} \delta_{\nu j} - \frac{1}{2} \delta_{\mu\nu} \delta_{ij}); \mu, \nu, i, j=1, 2.$$

Explicitly they are

$$A_1^1 = \begin{pmatrix} \frac{1}{2} & 0 \\ 0 & -\frac{1}{2} \end{pmatrix} \equiv I_3 \quad A_1^2 = \begin{pmatrix} 0 & 0 \\ 1 & 0 \end{pmatrix} \equiv I_-$$

$$A_2^1 = \begin{pmatrix} 0 & 1 \\ 0 & 0 \end{pmatrix} \equiv I_+ \quad A_2^2 = \begin{pmatrix} -\frac{1}{2} & 0 \\ 0 & \frac{1}{2} \end{pmatrix} \equiv -I_3$$

of which only three are independent, since  $A_1^1 + A_2^2 = 0$ . The right hand side justification will be more clear if we operate  $A_\nu^\mu$  on the doublet  $\begin{pmatrix} P \\ n \end{pmatrix}$ . It is interesting to see that  $A_\nu^\mu$  obey the commutation relation

$$[A_\nu^\mu, A_\rho^\lambda] = \delta_\nu^\lambda A_\rho^\mu - \delta_\rho^\mu A_\nu^\lambda.$$

Now we shall see in a moment that, besides the two dimensional representation of SU(2), we are able to find representations with different dimensionalities. The clue is to take the direct product of the doublet  $q$  with, say, a new doublet  $\bar{q}$  defined by

$$\bar{q} = \begin{pmatrix} \bar{p} \\ \bar{n} \end{pmatrix} \quad \text{with} \quad \begin{array}{ccc} I_3 & B & S \\ -\frac{1}{2} & -1 & 0 \\ \frac{1}{2} & -1 & 0 \end{array}$$

then we get

$$\bar{q} \times q = \begin{pmatrix} \bar{p}p & \bar{n}p \\ \bar{p}n & \bar{n}n \end{pmatrix} = \frac{1}{2}(\bar{p}p + \bar{n}n) \begin{pmatrix} 1 & 0 \\ 0 & 1 \end{pmatrix} + \begin{pmatrix} \frac{1}{2}(\bar{p}p - \bar{n}n) & \bar{n}p \\ \bar{p}n & -\frac{1}{2}(\bar{p}p - \bar{n}n) \end{pmatrix}$$

where the first part is an isospin singlet with  $I_3=0$ , and the latter is an isospin triplet with  $I_3 = -1, 0$ . Thus  $\bar{2} \times 2 = 1 + 3$ . By forming several direct products we construct irreducible representations of SU(2) with different dimensionalities. These are; 1, 2, 3, ...; that is

all integers.

### 1.6- THE GROUP SU(3)

As we saw, SU(2) has only two conserved quantities. But we have another conservation rule, namely the conservation of strangeness. In order to include it into the scheme we must extend SU(2). The simplest way of extending SU(2), as was proposed by Sakata in 1956, is to consider transformations on a new three component object (Sakaton):

$$q = \begin{pmatrix} p \\ n \\ \Lambda \end{pmatrix} \quad \text{with} \quad \begin{array}{ccc} I_3 & B & S \\ \frac{1}{2} & -1 & 0 \\ -\frac{1}{2} & -1 & 0 \\ 0 & 0 & -1 \end{array}$$

A rotation in the corresponding new hypercharge produces the transformation  $q \rightarrow Uq$ . Here too, U is unitary and unimodular. The set of these U matrices forms the group SU(3).

As before we would like to write U as

$$U = \exp\left(\frac{1}{2} \sum_{j=1}^8 \lambda_j \delta \theta_j\right),$$

where the generators of SU(3) are traceless, hermitian matrices. We shall call a linear combination of  $\lambda_j$  by  $A_\nu^\mu$  and define them as

$$(A_\nu^\mu)_{ij} = \delta_{\mu i} \delta_{\nu j} - 1/3 \delta_{\mu\nu} \delta_{ij}; \quad \text{with } i, j, \mu, \nu = 1, 2, 3.$$

Explicitly they are

$$A_1^1 = \begin{pmatrix} 2/3 & 0 & 0 \\ 0 & -1/3 & 0 \\ 0 & 0 & -1/3 \end{pmatrix} \equiv Q, \quad A_2^1 = \begin{pmatrix} 0 & 1 & 0 \\ 0 & 0 & 0 \\ 0 & 0 & 0 \end{pmatrix} \equiv I_+, \quad A_3^1 = \begin{pmatrix} 0 & 0 & 1 \\ 0 & 0 & 0 \\ 0 & 0 & 0 \end{pmatrix}$$

$$A_1^2 = \begin{pmatrix} 0 & 0 & 0 \\ 1 & 0 & 0 \\ 0 & 0 & 0 \end{pmatrix} \equiv I_-, \quad A_2^2 = \begin{pmatrix} 1/3 & 0 & 0 \\ 0 & 2/3 & 0 \\ 0 & 0 & -1/3 \end{pmatrix}, \quad A_3^2 = \begin{pmatrix} 0 & 0 & 0 \\ 0 & 0 & 1 \\ 0 & 0 & 0 \end{pmatrix} \equiv U_+$$

$$A_1^3 = \begin{pmatrix} 0 & 0 & 0 \\ 0 & 0 & 0 \\ 1 & 0 & 0 \end{pmatrix}, \quad A_2^3 = \begin{pmatrix} 0 & 0 & 0 \\ 0 & 0 & 0 \\ 0 & 1 & 0 \end{pmatrix} \equiv U_-, \quad A_3^3 = \begin{pmatrix} -1/3 & 0 & 0 \\ 0 & -1/3 & 0 \\ 0 & 0 & 2/3 \end{pmatrix} \equiv -Y$$

As there are two independent diagonal generators so we have two

conserved quantities. We define them as\*

$$\frac{1}{2}(A_1^1 - A_2^2) = \begin{pmatrix} \frac{1}{2} & 0 & 0 \\ 0 & -\frac{1}{2} & 0 \\ 0 & 0 & 0 \end{pmatrix} = I_3 \quad \text{"the third component of isospin"}$$

$$-A_3^3 = \begin{pmatrix} 1/3 & 0 & 0 \\ 0 & 1/3 & 0 \\ 0 & 0 & -2/3 \end{pmatrix} = Y \quad \text{"the hypercharge".}$$

The Gell-Mann-Nishijima relation links hypercharge with  $Q$  and  $I_3$ , this is

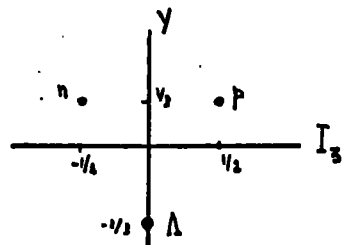
$$\begin{aligned} \text{where} \quad Q &= I_3 + \frac{1}{2}Y \\ Y &= B + S. \end{aligned} \quad (1.4)$$

Using the equation (1.4) we get the following

		Y	I	$I_3$	B	S	Q
q=	p	1/3	$\frac{1}{2}$	$\frac{1}{2}$	1/3	0	2/3
	n	1/3	$\frac{1}{2}$	$-\frac{1}{2}$	1/3	0	-1/3
	$\Lambda$	-2/3	0	0	1/3	-1	-1/3
$\bar{q}$ =	$\bar{p}$	-1/3	$\frac{1}{2}$	$-\frac{1}{2}$	-1/3	0	-2/3
	$\bar{n}$	-1/3	$\frac{1}{2}$	$\frac{1}{2}$	-1/3	0	1/3
	$\bar{\Lambda}$	2/3	0	0	-1/3	1	1/3

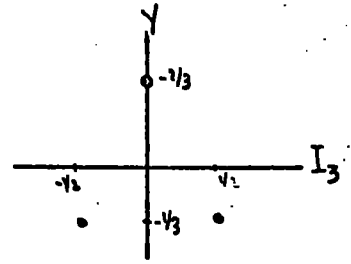
We see that  $q$  and  $\bar{q}$  do not correspond to physical particles since their  $Y$ ,  $B$  and  $Q$  are not integral. We shall call  $q$  and  $\bar{q}$  quark and anti-quark respectively, and the table above shows the properties of them. It is possible to show  $q$  and  $\bar{q}$  in a two dimensional plot, usually called a weight diagram :

Quark's weight diagram



\* In the original Sakata model the hypercharge was defined as  $Y = -A_3^3 + 2/3$  (See, e.g., Carruthers, 1966; page 37). As Sakata model has met several difficulties (e.g. the parity of the  $\Sigma$ ; see Hughes, 1972; page 206) we need not consider the early model. From now on we shall discuss the eight fold way.

Anti quark's weight diagram



A practical use of weight diagrams is in decomposing a direct product of representations to the irreducible ones. For example :

$$\bar{3} \times 3 = 1 + 8 .$$

This product is of special interest, since all the mesons found experimentally can be 'reproduced' by this method, in other words, mesons transform like quark-antiquark pair under  $SU(3)$ . Some examples are given in Table 1.

In the same way, we see that baryons can be constructed by  $qqq$

$$3 \times 3 \times 3 = 1 + 8 + 8 + 10.$$

Some examples are given in Fig. 7. This means that baryons are classified in singlets and octets like mesons as well as decuplets.

#### 1.6.1- Labeling of $SU(3)$

$I_+$ ,  $I_-$ ,  $I_3$  and  $Y$  form a subgroup  $SU(2)_I$  of  $SU(3)$ , since they satisfy the  $SU(2)$  commutation relations among themselves, and also commute with  $Y$ . Thus

$$SU(2)_I \times U(1)_Y \subset SU(3)$$

where  $U(1)_Y$  is simply the one element group. This indicates that  $SU(3)$  can be uniquely labelled by  $I^2$ ,  $I_3$  and  $Y$ .

Another alternative for labelling the group  $SU(3)$  comes from the fact that

$$SU(2)_U \times U(1)_Q \subset SU(3)$$

that is to label by  $U^2$ ,  $U_3$  and  $Q$ .

Another way of labelling is  $V$ -spin. Since, however, it is of no physical interest, we shall not consider it here. The properties

of I and U spins are easily understood from the commutation relations (Carruthers, 1966; page 38)

$$[I, Y] = 0$$

$$[U, Q] = 0$$

which, in turn, show that member of an I-spin multiplet have the same hypercharge and the members of U-spin multiplet have the same charge.

### 1.6.2- Mass Formula

Obviously pure SU(3) is broken by some unknown weaker mechanism but in such a way that I and Y are still conserved, since the masses of the particles in each representation are not equal. If one assumes the simplest form for the symmetry breaking interaction, then one can derive the Okubo mass formula for fermions and for bosons\* :

$$M = M_0 + M_1 Y + M_2 (I(I+1) - \frac{1}{4}Y^2)$$

$$m^2 = m_0^2 + m_2^2 (I(I+1) - \frac{1}{4}Y^2).$$

These formula give the Gell-Mann-Okubo mass relations for

baryon octet	$M_N + M_{\Xi} = 3\frac{1}{2}M_{\Lambda} + \frac{1}{2}M_{\Sigma}$	
pseudo scalar mesons	$m_K^2 = \frac{1}{4}m_{\eta}^2 + \frac{1}{4}m_{\pi}^2$	
vector mesons	$m_{K^*}^2 = \frac{1}{4}m_{\rho}^2 + \frac{1}{4}m_{\omega}^2$	" $\rho^8$ is mixture of , of the octet**."
baryon decuplet	$M_{N^*} - M_{Y_1^*} = M_{Y_1^*} - M_{\Sigma^*} = M_{\Sigma^*} - M_{\Omega}$	

We summarize some of the applications of SU(3) as follows :

1) Grouping of the particles and resonances into the SU(3) represen-

\* The use of the (mass) for fermions and the (mass)<sup>2</sup> for bosons in these formulae was suggested by R.P. Feynman. It is related to the fact that in the Lagrangian the mass term for bosons is  $m^2 \phi^\dagger \phi$  and for fermions  $M \bar{\psi} \psi$ .

\*\* The idea of mixing was proposed by Sakurai in 1962 who proposed also a mixing parameter in the form of the 'mixing angle'. The mixing parameters are :

$$|W\rangle = |V_1\rangle \cos \theta + |V_8\rangle \sin \theta$$

$$|W'\rangle = |V_8\rangle \cos \theta - |V_1\rangle \sin \theta$$

The mixing angles for the pseudo scalar mesons, vector mesons and

tations 1, 8, 10.

ii) Coupling of various particles together which yields relationships between coupling constants.

iii) Relations between the masses of the multiplets of each representation.

Finally, in order to get higher J mesons one can make use of orbital excitations. Generally higher excitations can be obtained by radial excitation, orbital excitation or by addition of  $\bar{q}q$  pairs. These excited states are all unstable against strong decays and are observed experimentally as resonances.

### 1.7- QUARKS, QUARK MODELS AND EXOTIC RESONANCES

What is a quark? Rubbish, trash, curd, filth,... are the equivalents that any German dictionary would give. The word 'quark' was taken by Gell-Mann\* for the first time in 1964. The name 'quark' essentially appeared when Gell-Mann and independently Ne'eman proposed an alternative, similar to that of Sakata, in classifying particles. In this model, as we saw earlier, the particle structure is expressed in terms of the allowed values of isospin and strangeness using the three basic objects having baryon number  $B=1/3$  and third integral electric charges. These strangely established 'particles\*\*' are playing the roles of 'building blocks!'. Since mesons and baryons can be constructed by the combination of quarks and antiquarks, that

---

→ tensor mesons are  $+10^0_4$ ,  $+39^0_9$  and  $+29^0_9$  respectively. These mix  $(\eta, \eta')$ ,  $(\omega, \phi)$  and  $(f, f')$ .

\* The word 'quark' was taken by Gell-Mann from James Joyce's novel 'Finnegan's Wake'.

\*\* We shall consider quarks to be physically existing particles. Although lots of theories have been given in which no assumptions has been made on their presence, and even no experiments so far has been successful to trap them, there is still no reason why they should not exist. Their failure in showing up themselves in experiments does not mean anything except that they are not found by these experiments!

$\bar{q}q$  and  $qqq$  respectively. Quarks are strongly interacting particles. We would expect quarks to be surrounded by meson clouds like other hadrons. However some simple predictions, for example the approximate ratio of  $\mu_p / \mu_n = 3/2$  for the proton, neutron magnetic moments follow simply from the assumption that the quarks have just their Dirac magnetic moments (Morpurgo 1969).

The assumption that baryons are made of three spin  $\frac{1}{2}$  objects suggests the conclusion that the lowest lying baryon states must have spin a half and three halves and the same parity in agreement with experiment. Examination of the quantum numbers of experimentally observed resonances shows that they are limited to those values predicted by this naive quark model. States with forbidden quantum numbers are called exotic. The exotic resonances are not in one or eight representations for mesons and not in one, eight or ten representations for baryons There are three kinds of exotic states\*. These are

- i) Mesons or baryons with IBY values not found in the quark anti-quark or three quark systems. This is usually referred to as exotic states of the first kind.
- ii) Mesons with odd CP and natural parity, and  $0^{--}$  mesons (exotic states of the second kind).
- iii) Baryons with unnatural orbital parity  $P = (-)^{L+1}$ , where L is the total orbital angular momentum of the quarks (which of course is not 'observable' and depends upon the model). See Lipkin (1970).

If exotic states exist, then for a given spin, they lie higher in mass and couple less strongly to the known channels than non-exotic resonances. Their absence in a reaction implies constraints on the imaginary parts of the scattering amplitude in crossed chan-

---

\*There is another type of exotic state when taking SU(6) into consideration. As we did not and shall not talk about SU(6), therefore we should not worry about it.

nels. These constraints, in terms of duality diagrams, are represented by direct lines corresponding to their quark and antiquark content, lines cannot change their character or double back on themselves, and legal diagrams contain two lines and three lines in mesonic and baryonic channels respectively.

The absence of exotic states has been used as an input in theoretical calculations with super-convergence and FESR\* to obtain a number of interesting results. Their absence is introduced into the sum rules

$$\int_0^N y^n \text{Im } A(y, t) dy = f_n(N, t) \quad 0 \leq n \leq N$$

by setting the left hand side equal to zero for sum rules with exotic s-channel quantum numbers, and the right hand side equal to zero for channels having exotic t channel quantum numbers.

Some indirect evidence against exotic resonances can be found from the absence or presence of forward or backward peaks in the angular distribution of certain reactions :

Two body reactions lead in general to both a forward peak and a backward peak, usually interpreted as being due to meson and baryon exchange respectively. Now what one can observe is that both in meson and in baryon exchange the corresponding forward or backward

---

\* See the duality chapter.

peak disappears whenever it would correspond to the exchange of an exotic particle. This is shown in figures 8, 9, 10. However, the quark model offers the only description for the absence of the exotic states so far.

Much effort has been given into correlating the spectrum obtained from quarks and all the observed hadron states, particularly the baryons. This has achieved considerable success although some obscurities remain. We refer to the recent review by Dalitz (1973) for details.

The situation of the quark model is as follows.

- i) The outstanding success of the quark model has been in defining the exotic states.
- ii) The model has been used to obtain many results which are in good agreement with experiment : resonance spectroscopy, high energy scattering and reactions, electromagnetic and weak coupling. All of these are in the domain of IBY Physics (i.e. symmetries), (Lipkin, 1969).
- iii) No useful results in the domain of stu Physics (dynamics) have been obtained from the quark model, e.g. interactions, scattering amplitudes are known and are considered as free parameters in any dynamical calculations.
- iv) There is no theoretical prediction for the mass of the quark.

The success of the predictions indicate at least that the quark model has an underlying algebraic structure which is relevant to hadron physics. Whether it is only the algebraic structure of the model which is relevant or whether there are real physical quarks is still not clear at present. If the quarks exist they answer one question about the regularities in the observed quantum numbers of the low lying hadron spectrum. But they pose a new question: Why do all the observed hadron states have integral charge and baryon number ?

We end up this chapter by drawing a quark diagram of  $MB \rightarrow MB$ ,  
Fig 32(b), (for a detailed discussion see chapter three).

The selection rule obtained from this figure is : If only one  
quark in a baryon is responsible for the transition producing  
a resonance, the two other quarks are 'spectators' and must re-  
main in the same state in the resonance as in the initial baryon.

This is in good agreement with experiment.

\*\*\*\*\*

!!!!!!

..

.

## CHAPTER 2

### $A_1$ and the Deck effect

The reaction  $\pi^+p \rightarrow \pi^+\pi^-\pi^+p$  was studied at 3.65(Gev/c) by Goldhaber et al in 1964. They observed an anomaly in the mass distribution of the  $\rho\pi$  system. Their result indicated that the majority of the events involved some resonance phenomenon between the outgoing particles, through different intermediate channels (Table 2). The most prominent feature of the  $M(\pi^+\pi^-)$  distribution was  $\rho^0$  production (Figure 11) defined by  $0.65 \sqrt{M(\pi^+\pi^-)} \leq 0.85$  Mev. These events proceed with comparable cross sections through the channels  $\pi^+p \rightarrow \rho^0 + N^{*++}$  and  $\pi^+p \rightarrow \rho^0\pi^+p$ . In the second channel, 1b, the formation of  $\rho^0$  mesons proceeds via large momentum transfers to the pion-nucleon system. It was in this channel that a strong enhancement in the distribution of  $M(\rho^0\pi^+)$  in the mass region 1.00 to 1.40 Gev was observed. They referred to this enhancement as the formation of a state  $A^+$  according to  $\pi^+p \rightarrow A^+$  which breaks up as  $A^+ \rightarrow \rho^0\pi^+$ . In figure 12 the projection of events, excluding the  $N^{*++}$  band, on the  $M^2(\rho^0\pi^+)$  has been shown. It was in this projection that the  $A^+$  enhancement effect over phase space predictions was noted. It is noteworthy that all of the  $\pi^+\pi^-$  mass doublets inside the  $\rho^0$  band (double  $\rho$  events) contribute considerably to the  $A^+$  enhancement. This raises the question whether the  $A^+$  enhancement might be related to a dynamical effect favouring double formation. Note that the  $A^+$  state is produced with small four momentum transfer to the proton,  $\Delta^2$ . In figure 13 the peaking at small values of  $\Delta^2$  for the region of the  $A^+$  enhancement is evident. Also peaks in the  $3\pi$  mass dis-

tribution had been represented for the first time in a similar region by Bellini et al (1963). A possible interpretation of the observation is that there is a resonance in the  $\pi^+\rho^0$  system. Then the relevant parameters as had been estimated were (Goldhaber et al, 1964);  $E_{A^+}=1.2$  Gev,  $\Gamma_{A^+}=0.35$  Gev, G-parity=-1, I=1 or 2 (see later this discussion).

Further investigations showed that what was previously reported as one resonance was in fact, two resonances. Chung et al (1964) studied the  $\pi\rho$  interaction in  $\pi^-p \rightarrow \pi^+\pi^-\pi^-p$  and found that the  $\pi^-\pi^+\pi^-$  effective mass distribution showed two clearly resolved peaks above the  $3\pi$  phase space background. This is shown in Fig 14. The first peak is at 1090 Mev with full width  $\Gamma \approx 150$  Mev, the second at 1310 Mev with  $\Gamma \approx 80$  Mev. These two peaks nowadays are referred to as  $A_1$  and  $A_2$  respectively. It has been suggested that the first peak,  $A_1$ , arises from the kinematical effect, as we shall discuss in a moment, and the second one,  $A_2$ , is a true resonance.

### 2.1- THE DECK EFFECT

The discussion of this effect was stimulated by the discovery of the  $A_1$  meson as a peak in the  $\pi\rho$  spectrum near  $\pi\rho$  threshold. In his earlier work, Deck suggested the diagram of Fig 15 to explain the state enhancement. There, he assumes that the reaction  $\pi^+p \rightarrow \pi^+\rho p \rightarrow \pi^+p\pi^+\pi^-$  proceeds principally via peripheral collisions which are dominated by one pion exchange (OPE). The cross section associated with Fig 15 is (Deck, 1964),

$$\frac{d\sigma}{du^2} = \left(\frac{g^2}{4\pi}\right) \frac{m^2 - 4m^2}{4F_I^2} \left(\frac{d\sigma}{d\Omega}\right)_0 \int_{-t_{\min}^2}^{-t_{\max}^2} d(-t^2) \int_{\omega_0^2}^{\omega_{\max}^2} d\omega^2 e^{-\lambda(-t^2)} \frac{1}{B} \frac{\Omega}{u} \frac{(-\omega^2)}{(a - b/B(A - \omega^2))^2} \quad (2.1)$$

where

$F_I = M_1 m_\pi p_2$  is the invariant flux,

$g^2/4\pi \approx 1.8$  is the  $\pi\pi\rho$  effective coupling constant,

$$\omega^2 \equiv (q + q_1)^2 = A - B \cos\theta_2 + c \sin\theta_2 \cos\phi_2$$

$\approx A - B \cos\theta_2$  is the square of total c.m. energy of the  $\pi\rho$  system,

$\lambda$  appears when we approximate  $\frac{d\sigma_{\pi N}}{d\Omega} = \left(\frac{d\sigma}{d\Omega}\right)_0 \exp(\lambda t^2)$ ,

$$t^2 = (q_1 - p_1)^2,$$

$$u^2 = (q + q_2)^2,$$

$$(-t^2)_{\max} = -2W^{-2}((W^2 - M_1^2)^2 - m^2(W^2 + M_1^2) - (W^2 + M_1^2 - m^2) u^2 +$$

$$(W^2 - 2(M_1^2 + m^2) W^2 + (M_1^2 - m^2)^2)^{\frac{1}{2}} (u^4 - 2(W^2 + M_1^2) u^2 + (W^2 - M_1^2)^2)^{\frac{1}{2}}),$$

$$W^2 = (p_1 + p_2)^2,$$

$a, b, A, B$  and  $c$  are positive functions of  $W^2$ ,  $u^2$  and  $t^2$ ,

$$\omega_{\max}^2 = A + B,$$

$$\omega_0^2 = \text{some constant} = 2.70 \text{ Gev}^2,$$

$\theta_2, \phi_2$  are the spherical angles of  $q_2$  relative to  $p_2$  at  $q, q_2$  center of mass system. The other notations are given in Fig 15.

In deriving (2.1) these approximations have been made :

i) On mass shell  $M_{\pi N}$  have been equated by the off mass shell amplitude  $M_{\pi N}^i$ .

ii)  $\omega^2 \approx A - B \cos\theta_2$ .

iii)  $\omega$  is supposed to be sufficiently high;  $\omega^2 < \omega_0^2$  are excluded from these calculations ( $\omega_0^2 = 2.70 \text{ Gev}^2$ ).

The solid curve of Fig 16 represents a plot of  $d\sigma/du^2$  as a function of the center of mass energy of the  $\pi\rho$  system for  $\lambda = 6 (\text{gev}/c)^{-2}$ ,  $p_2 = 3.65 \text{ Gev}/c$  and  $\omega_0^2 = 2.70 (\text{Gev})^2$ . Note that the shape of the function  $d\sigma/du^2$  is rather insensitive to the value chosen for  $\omega_0$ , and that as

the incident pion momentum is increased the peak should become larger and broader, in other words, peaks are energy dependent. Fig. 17 is a sketch of the data of Goldhaber et al (1964) at the pion laboratory momentum cited above. The total cross section obtained in this way is about  $\frac{1}{2}$  mb, which is almost 30 times smaller than the experimental value.

Later in 1965, Maor and O'Halloran improved the calculations of Deck, simply by removing the third approximation cited above (only the events with values of  $u$  in the  $N^*$  resonance band were excluded). Figure 18 represents their calculated mass spectrum of  $u^2$ , with  $p_2=3.65$  Gev/c. The estimated total cross section was .22 mb. And as Deck had shown, the calculated peaks did not fall in definite angular or isotopic spin states. More improvement came when the second approximation was removed by Deutschmann et al (1966). Their result showed that in this way broader peaks at the higher momenta were produced and that the position of the peak was always at about 1100 Mev, independently of incoming energy but that the width of the peak increased with increasing energy.

A better more realistic OPE diagram in studying the same reaction was given by Aderholz et al (ABBBHL Collaboration, 1965) (Fig. 19). A comparison of the model with the available data has been made in Fig. 20. These curves reproduce the general shape of the distributions quite well. In the  $A_1$  region the OPE model gives a peak which is not as narrow and as high as the experimental one.

So far all the discussions were on the basis that the  $A_1$  is a kinematical enhancement (as the OPE models indicate). The fact that the  $A_1$  enhancement has not been seen in other modes, though others are energetically possible, give additional weight to the idea that

~~it is not a resonance~~. But soon afterwards Deutschmann et al presented results from a study of 8 GeV/c  $\pi^+p$  interactions which were not compatible with the interpretation of the  $A_1$  as a kinematical effect. Their result is shown in Fig 21. There, the experimental distribution was fitted with two Breit-Wigner curves for the two enhancements plus a background (the solid line). The peak observed at  $1076 \pm 14$  Mev contains sixty per cent of the events in the  $A_1$  region and the presence of this peak above background is consistent with the description of the  $A_1$  as a resonance (The remaining forty per cent is the background).

Another improvement in Deck's model appears when one Reggeizes the exchanged pion. This has been done by Berger (1968). The basic assumption he makes is that  $\pi N \rightarrow \pi p N$  proceeds primarily via doubly peripheral collisions (Fig 22), where  $\bar{I}$  and  $\bar{II}$  are Regge pole exchanges and corresponding trajectories are  $\alpha_{\bar{I}}, \alpha_{\bar{II}}$ . The amplitude relevant to the figure, supposing the pion is exchanged in the second leg and a non Regge exchange for the first one (the pomeron can be exchanged here), is

$$|M|^2 = g^2 (m_p^2 - 4m_\pi^2) \lambda_0 (\pi \sigma_{\pi N}(s_1))^2 (1 + \alpha)^2 \exp(At_1) \frac{\beta(t_2)}{2(1 - \cos \alpha)}$$

$$\left( \frac{1}{s_0} (s_2 - t_1 - m_\pi^2 - \frac{1}{2t_2} (m_p^2 - m_\pi^2 - t_2)(t_1 + t_2 - m_\pi^2)) \right)^{2\alpha_\pi},$$

where

$$s_1 = (q + q_1)^2, \quad s_2 = W^2 = (q + q_2)^2, \quad t_1 = (q_1 - p_1)^2, \quad t_2 = (q_2 - p_2)^2,$$

$$\lambda_0 = (s_1 - (m_N - m_\pi)^2)(s_1 - (m_N + m_\pi)^2),$$

$g^2/4\pi \approx 2.2$  is the effective  $\pi\pi p$  coupling constant,

$\alpha_\pi$  is the pion trajectory,

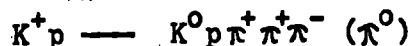
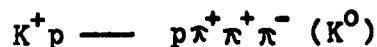
$\beta(t_2)$  is a smooth function normalized to unity at  $t_2 = m_\pi^2$ ,

$\sigma_{\pi N}(s_1)$  is fixed at 29mb.

Figure 23 shows the comparison of the results of the Deck and Berger type calculations for two different incident pion momenta.

## 2.2- OTHER EXPERIMENTS

The  $A_1$  has been produced in many other reactions. Figure 24 shows the  $\pi^+\pi^-\pi^-$  mass spectrum from the reaction  $\pi^-p \rightarrow p\pi^+\pi^-\pi^-$  at 16 GeV/c where the  $A_1$  is observed (French, 1968). In figure 25 the result of Anderson et al is shown where they have studied  $\pi^-p \rightarrow pB^-$  at an incident momentum of 16 GeV/c ( $B^-$  is the missing mass meson with negative charge). The enhancement near the  $A_1$  region is clear. Their calculations show that the  $A_1^-$  has mass  $M = 1.115 \pm 0.020$  GeV/c<sup>2</sup> and  $\Gamma = 0.098 \pm 0.045$  GeV/c<sup>2</sup>. The other experiment performed by Grennell et al (1970) shows a well defined peak at 1120 MeV which is also consistent with a  $\rho^0\pi^-$  decay mode and which is well separated from the  $A_2$  (Fig 26). Their estimate of  $\Gamma$  varies from 100 to 300 MeV according to what value the background is assumed to take. A calculation made by Nasrollah (1970) to compute the width of the  $A_1$  meson from current algebra gives  $\Gamma = 75$  MeV. The other observations of the  $A_1$  have been made in the reactions



at energies between 9 and 12.8 GeV/c. But the test made by Rabin et al (1970) showed no  $A_1$  bump in any of these four reactions. This casts doubt on the conclusion of the observation of the  $A_1$  in these

reactions. It is interesting to quote that a bump between the  $A_1$  and the  $A_2$ , usually denoted by  $A_{1.5}$ , has been reported which has a mass of about 1190 Gev (Lamsa et al, 1968). Abolins et al strengthen the assignment of the isospin of the  $A_1$  to be one (Abolins et al, 1966).

The  $A_1$  mainly decays into  $\pi\rho$  but  $A_1 \rightarrow \pi\pi$  is also possible and proceeds via p-wave ( $\pi$  is the s-wave daughter of  $\rho$ ). But, so far this decay has not been seen experimentally.

To close this section we quote the discussion of Roberts (1971): The close similarity of the energy dependence of the cross sections for  $A_1$  and  $A_2$  production, Fig 27, suggests that since  $A_2$  is well known to be produced by  $\rho$ -f exchange, then the possibility of the same exchange generating the  $A_1$  seems likely.

### 2.3- THE $A_1$ NONET

A nonet with  $J^{PC}=1^{++}$  in  $A_1$  mass region fits well into the quark model  ${}^3P_1$  ( $L=S=1$ ). We call this the ' $A_1$  nonet'. There are candidates for the other members of the nonet, but none of them are certain (Table 3). The  $\rho$  is also contaminated by kinematic background, while the spin-parity of the  $I=0$  candidates, i.e.  $D(1285)$  and  $D'(1422)$  is not well determined. There have been suggestions for the  $M(953)$  as another possible candidate, In Table 4 the decay modes of the  $A_1$  nonet have been given. Table 5 is devoted to  $A_1$  nonet cross sections.

### 2.4- ARGUMENTS ON THE $A_1$ AND ITS FUTURE

In the final section of the chapter we summarize the arguments for the  $A_1$  being a resonance and/or background. At the end we will have some discussion on the  $A_1$ 's future. In the next chapter, after introducing the idea of duality, we shall see what duality says about the different interpretations of the  $A_1$ .

#### 2.4.1- Arguments For A Resonance.

1) Quark model. As discussed above.

#### 2.4.2- Arguments For Kinematic Enhancement (Diebold, 1972).

i) Good fits. Reggeized Deck calculations can give good agreement with the many mass distributions observed.

ii) Helicity conservation. The angular distributions for kinematic effects give approximate t-channel helicity conservation. If the enhancement were a resonance, one might have expected s-channel helicity conservation. This argument has a weak spot, since  $\pi \rightarrow A_1$  may

be different from these processes because of the spin change  $0^- \rightarrow 1^+$ .

iii) Possible  $0^-$  enhancement. The  $0^-$  p-wave  $\rho\pi$  distribution peaks up at low mass with roughly the same shape as the  $A_1$ , but only 10 or 15 per cent of the intensity. One interpretation of this effect is that the Deck diagrams are contributing to more than just the s-wave. One might also imagine that through some inadequacy in analysis a small fraction of the  $1^+$  events are leaking into the  $0^-$  results.

#### 2.4.3- The Future Of The $A_1$ .

It seems clear that any definitive study of the  $1^{++}$  resonances predicted by the quark model is going to have to come from channels with reduced background. Such channels are more difficult to find than one might imagine. There have been suggestions that hypercharge exchange reactions such as  $K^-n \rightarrow A_1^- \Lambda$  may be the best place to look for an  $A_1$  resonance. Or, as Fox and Hey (1973) have proposed one can search in photon induced processes. Its expected cross section can be estimated reliably by a pole extrapolation; failure to observe it with the predicted size would be unambiguous evidence against its existence (the cross section for  $\gamma p \rightarrow A_1^+ n$  at  $E = 4.7$  Gev

is  $0.5\mu\text{b}$ ). However there is no report of  $\bar{p} \rightarrow A_1^+ n$  as yet. Another experimental test for the  $A_1$  has been long ago proposed by Rosenfeld (1965). He shows that if the  $A_1$  is a true resonance, and if there is not too much interference in its decay, then

$$\begin{array}{ccccccc} \pi^+ d \rightarrow p p \bar{p} \pi^+ & : & \rho^+ \pi^- & : & \rho^0 \pi^0 & : & \pi^+ p \rightarrow p \rho^0 \pi^+ & : & \pi^- p \rightarrow p \rho^0 \pi^- \\ \frac{1}{2} & : & \frac{1}{2} & : & 0 & : & \frac{1}{2} & : & \frac{1}{2} \end{array}$$

By contrast, if the  $A_1$  bump results from the OPE diagram then we expect

$$0 : \sigma_1 : \sigma_1 : \sigma_2 : \sigma_3$$

where  $\sigma_1$ ,  $\sigma_2$  and  $\sigma_3$  are the experimentally known  $\pi N$  scattering cross-sections:  $\sigma_1(\pi^+ n \rightarrow \pi^0 p)$ ,  $\sigma_2(\pi^+ p \rightarrow \pi^+ p)$ ,  $\sigma_3(\pi^- p \rightarrow \pi^- p)$  respectively.

\*\*\*\*\*

!!!!!!!

@@@

.

## CHAPTER 3

### Duality

What is duality ? The term 'duality' appeared in physics about half a century ago. There, it was used to clarify the concept of wave-matter connection. This is named 'old duality' these days. The 'new duality' is almost six years old. This connects the description of the scattering amplitude in two different channels as we shall discuss now.

Duality expresses the relation between two descriptions of the hadronic scattering amplitude : At low energy the description by direct channel resonances is simple and useful (Fig 28(a)). At low energy the data show prominent peaks as a function of energy, and one can try the approximation of resonance saturation, that is, of neglecting the non resonating background. The second description is the exchange of Regge poles, and is useful at high energy where typical features are forward peaks and energy dependence  $s^\alpha$  (Fig 28(b)). The two descriptions are very different; resonance formation corresponds to poles in the  $s$  channel, Regge exchange to poles in the  $t$ -channel. Duality says that there are direct relations between these two descriptions, that they are equivalent in a certain sense. Each of the two descriptions is by itself an approximation to a complete-description (Table 6). The controversy arises only when one makes approximations.

Duality takes its most precise meaning in the framework of finite energy sum rules (FESR). They are consistency conditions im-

posed by analyticity on functions that can be expanded at high energies ( $\gamma \gg N$ ) as a sum of Regge poles. Let us see how one can derive FESR for the two particle processes;

It is convenient to use the variables  $\gamma = \frac{s-u}{4m}$  and  $t$ , where  $m$  is the mass of the target. The amplitudes  $A^\pm(\gamma, t)$ , even or odd under  $(s-u)$  crossing ( $\gamma \rightarrow -\gamma$ ), are assumed to satisfy fixed  $t$  dispersion relations in :

$$A^\pm(\gamma, t) = \frac{1}{\lambda} \int_0^\infty d\gamma' \operatorname{Im} A^\pm(\gamma', t) \left( \frac{1}{\gamma - \gamma'} \pm \frac{1}{\gamma' + \gamma} \right) \quad (3.1)$$

where the  $\gamma'$  integral has discrete (pole) contributions for  $0 < \gamma' < M$  and continuum contributions for  $\gamma' > M$ . Equation (3.1) is equivalent to Cauchy's theorem applied to a function that is analytic in the cut  $\gamma$  plane, apart from isolated poles on the real axis. Now, suppose that for  $|\gamma| > N$ ,  $A^\pm(\gamma, t)$  can be written as an expansion in Regge poles (or power law terms) :

$$A^\pm(\gamma, t) = R^\pm(\gamma, t) \quad (|\gamma| > N)$$

where

$$R^\pm(\gamma, t) = \sum_j \beta_j(t) \gamma^{\alpha_j(t)} \cdot \left( \frac{1 - \cot \frac{1}{2} \pi \alpha_j}{1 + \tan \frac{1}{2} \pi \alpha_j} \right),$$

then the difference  $\Delta(\gamma, t) \equiv A(\gamma, t) - R(\gamma, t)$  satisfies (3.1) and vanishes for  $|\gamma| > N$ . Furthermore the integral on the right hand side of (3.1) vanishes for  $\gamma' > N$ . By considering  $\gamma > N$  and expanding the denominators in  $\gamma'/\gamma$ , this dispersion relation for  $(\gamma, t)$  yields the set of integer moment FESR :

$$\int_0^N d\gamma \gamma^n \operatorname{Im} A^\pm(\gamma, t) = \int_0^N d\gamma \gamma^n \operatorname{Im} R^\pm(\gamma, t) \quad (3.2)$$

where  $n=0, 2, 4, \dots$  for  $A^-$  and  $n=1, 3, 5, \dots$  for  $A^+$ . Since the right hand side of (3.2) involves only powers of  $\gamma$ , the integral can be

done explicitly and one finds

$$S_n \equiv N^{-n-1} \int_0^N dy y^n \text{Im} A^\pm(y, t) = \sum_j \frac{\beta_j(t) N^{\alpha_j(t)}}{\alpha_j(t) + n + 1}. \quad (3.3)$$

This is the so called finite energy sum rule relation and relates the low energy properties of a scattering amplitude, expressed as an integral up to  $y=N$ , to the high energy properties in terms of Regge poles (or perhaps something more complicated). The exchange Regge trajectories can be considered as built up from direct channel resonances. Conversely, Regge exchange already includes the resonances in an average sense. This is the Dolen, Horn, Schmid (1967,1968) duality also referred to as global and average duality. It is interesting to note that if a secondary pole or a cut is unimportant in a high energy fit above  $N$ , then this singularity is unimportant to exactly the same extent in the low energy sum rules for the various moments. In brief, therefore, resonances in the  $s$  channel and Regge poles in the  $t$  channel appear as two complementary ways to describe a two body amplitude. FESR are not restricted to cases where the amplitude is convergent at infinity. It is only necessary that the amplitude should have a known asymptotic behaviour. It is of course obvious that FESR cannot tell us whether a given singularity is a pole or a cut, they are, however, useful in distinguishing between particular specific models.

It is possible to deduce  $\alpha(t)$  from the ratios of different moment sum rules directly

$$\frac{S_n(t)}{S_m(t)} = \frac{\alpha(t) + m + 1}{\alpha(t) + n + 1}$$

that is,  $\alpha(t)$  can be deduced by taking the first two nonvanishing

moments. It is advisable to work separately with the odd and the even moment sum rules, since one of these families contains the wrong signature nonsense poles that do not affect the observable amplitude. Once  $\alpha(t)$  is determined, one can go on and determine  $\beta(t)$  from the various  $S_1$ .

An advantage of the FESR method over conventional fits is that the input amplitudes, e.g. the  $A'$  and  $B \widehat{N}$  amplitudes, are already decomposed into their spin components, whereas the high energy  $d\sigma/dt$  data only enables us to find  $A'^2$  and  $B^2$ , and the signs of the amplitudes cannot be determined.

### 3.1- DUALITY AND INTERFERENCE MODEL

Earlier than the time duality was proposed, an alternative description for the scattering amplitudes in the intermediate energies had been introduced which was named the 'interference model'. The interference model represents the scattering amplitude  $F$  as the sum of direct channel resonance amplitude  $F_{res}$  and crossed channel exchange amplitude  $F_{Regge}$  (Fig. 29) in the intermediate energy region (Barger and Cline, 1967),

$$F = F_{res} + F_{Regge} .$$

In contrast, Dolen et al (1968) show that the correct prescription should be,

$$F = F_{res} + F_{Regge} - \langle F_{res} \rangle ,$$

where  $\langle F_{res} \rangle$  denotes the locally averaged resonance amplitude. As it is seen the term  $\langle F_{res} \rangle$  has not been included in the interference model. If all resonances enter with the same sign, then  $\langle F_{res} \rangle \neq 0$  and the interference model involves double counting. On the other hand, if the resonances enter with alternating signs and com-

parable strength, then  $\langle F_{res} \rangle \neq 0$  and the interference model agrees with the duality prescription. A similar argument can be found elsewhere (Schmid, 1970).

### 3.2- APPLICATION OF FINITE ENERGY SUM RULES

There are three ways in which one can use the FESR;

- i) One can use the information about the Regge terms implied from the high energy data as an input in order to determine parameters of the s channel resonances.
- ii) Similar to (i) but to use the low energy data as an input to predict the exchanged Regge poles.
- iii) Various sum rules can be used together with the high energy data to provide a better over-all determination of the Regge parameters.

### 3.3- DUALITY AND ITS EVOLUTION

- i) Schmid's calculation (1968) of the s channel partial wave projections of  $B^-$  amplitude given by  $\rho$ -exchange yielded resonance like circles on the Argand diagram as was discussed in chapter 1.
- ii) Exchange degeneracy. It is well known in potential scattering that the presence of Majorana exchange forces causes the force to be different in even and odd l states, giving rise to two distinct families of bound states or resonances. Conversely, the absence of exchange forces implies that states with even and odd l values can be treated together. In the language of Regge poles this means that trajectories will be exchange degenerate, with even and odd signature poles really being one Regge pole. In other words, the absence

of resonance in one channel implies the coincidence of exchanged trajectories with opposite signatures and a relation between their residue functions. The assumption of exchange degeneracy for the mesons correlates well with the presence or absence of resonances in the direct channel.

iii) The special role of the pomeron Regge pole. From the empirical observations that the differential cross section  $d\sigma/dt$  is closely proportional to  $s^{-a}$  which in turn implies that all the amplitudes are essentially real at high energies ( $a \in \mathbb{N}$ ), Harari in 1968 made the conjecture that for all processes the normal Regge trajectories ( $P', \rho, \omega, A_2$ ) are associated, in the sense of FESR and duality, with the direct channel resonances alone, and the pomeron is associated with only the background (Harari, 1970). Evidence in support of Harari's idea comes from the phase shift analyses of  $\pi N$  scattering (Jackson, 1969; 1970).

#### 3.4- THE VENEZIANO MODEL

An explicit crossing symmetric function, which satisfies the FESR and exhibits duality, has been given by Veneziano (1968). For simplicity we shall discuss the Veneziano representation for the s channel  $\pi^+ \pi^- \rightarrow \pi^+ \pi^-$  amplitude. In this case the t channel is identical to the s channel, and the u channel is exotic ( $I=2$ ). Once the pomeron contribution has been removed we expect the leading contribution to be the  $\rho$ -f exchange degenerate trajectory in both channels.

The simplest functional form which has an infinite set of s-channel poles lying on a trajectory  $\alpha_s(s)$ , with the poles appearing when  $\alpha_s \in \mathbb{N}$ , is  $\Gamma(1-\alpha_s(s))$ . Since an identical behaviour in the t-channel is required one can try

$$A(s,t) = \Gamma(1 - \alpha_s(s)) \Gamma(1 - \alpha_t(t)),$$

but this would have a double pole at every  $s - t$  point where both  $\alpha_s$  and  $\alpha_t$  are integral. It is easy to remove these poles by dividing by

$$V(s,t) = g \frac{\Gamma(1 - \alpha_s(s)) \Gamma(1 - \alpha_t(t))}{\Gamma(1 - \alpha_s(s) - \alpha_t(t))}$$

where  $g$  is an arbitrary constant giving the scale of the couplings. This function has pole lines at fixed  $s$  and at fixed  $t$ , where the  $\alpha$ 's are integers, and lines of zeros running diagonally through the intersections of the poles (Fig 30). In deriving the Veneziano model, besides exchange degeneracy, a zero width approximation is assumed (i.e. resonances are approximated by poles on the real axis).

The asymptotic behaviour of the model may be obtained by means of

$$\Gamma(x) \xrightarrow{x \rightarrow \infty} (2\pi)^{\frac{1}{2}} e^{-x} x^{x-\frac{1}{2}}$$

$$\Gamma(x) \Gamma(1-x) = \pi / \sin \pi x,$$

which yield :

$$V(s,t) \longrightarrow \frac{\pi(\alpha_s(s))^{\alpha_t(t)}}{\Gamma(\alpha_t(t)) \sin(\pi \alpha_t(t))} e^{-i\pi \alpha_t(t)}$$

So, if  $\alpha_s(s)$  is a linear function of  $s$ ,  $\alpha_s(s) = (0) + \alpha' s$ , we end up with Regge behaviour

$$V(s,t) \sim (\alpha' s)^{\alpha_t(t)}.$$

The asymptotic form of the amplitude displays several features. The first is the power law behaviour  $s^{\alpha_t(t)}$  as just mentioned. The second is the specification of the scale parameter  $s_0$  in  $(s/s_0)^{\alpha_t(t)}$  as the reciprocal of the slope of the trajectory. The third feature is the presence in  $V(s,t)$  of the phase  $\exp(-i\pi \alpha_t(t))$  as expected from

duality argument. A final aspect is the factor of  $\alpha(t)$  in the numerator. This is the 'ghost killing' factor that eliminates a particle of  $J^P=0^+$  from the leading trajectory.

However interesting and useful the Veneziano amplitude is, there are two important drawbacks of the Euler B function (Jacob, 1969) :

$$B(\alpha(s), \alpha(t)) = V(\alpha(s), \alpha(t)) = \int_0^1 x^{-\alpha(s)-1} (1-x)^{-\alpha(t)-1} dx \quad (3.4)$$

$$= \frac{\Gamma(-\alpha(s)) \Gamma(-\alpha(t))}{\Gamma(-\alpha(s) - \alpha(t))} \quad (3.5)$$

i) The satellites. One can add arbitrary regular function of  $x$  to the integrand of (3.4) such as

$$B'(\alpha(s), \alpha(t)) = \int_0^1 f(x) dx x^{-\alpha(s)-1} (1-x)^{-\alpha(t)-1}$$

without having altered the properties of the model. This is equivalent to write

$$B'(\alpha(s), \alpha(t)) = C_{00} B + \sum_{N,M} C_{NM} \frac{\Gamma(N-\alpha(s)) \Gamma(M-\alpha(t))}{\Gamma(N+M-\alpha(s)-\alpha(t))} .$$

These many possible terms, which differ from the leading one (3.5) by the fact that the first few poles in  $s$  or (and)  $t$  are missing, are called satellites. There is at present no way to limit this ambiguity in any general sense.

ii) The unitarity problem. At present it is impossible to remedy the incompatibility of (3.4) with unitarity in any fully satisfactory way.

### 3.5- DUALITY DIAGRAMS

The ramifications of duality and the absence of exotic resonances in all channels can be codified neatly by means of duality diagrams (Harari, 1969; Rosner, 1969). The rules for drawing a legal diagram are extremely simple :

- i) There are three types of lines corresponding to  $p$ ,  $n$ ,  $\lambda$  quarks. Lines do not change their identity.
- ii) Every external baryon is represented by three lines running in the same directions.
- iii) Every external meson is represented by two lines running in the opposite directions.
- iv) The two ends of a simple line cannot belong to the same external particle.
- v) In any  $B=1$  channel ( $s, t$  or  $u$ ) it is possible to cut the diagram into two, by cutting three quark lines. Similarly, in any mesonic channel we should be able to split the diagram by cutting only two lines.

If the diagram can be drawn so that no lines cross, the diagram is said to be planar and exhibits duality in the two channels (Fig 31). If the diagram contains lines that cross, it is non planar and will possess intermediate states that are exotic. Planar duality diagrams lead to high energy amplitudes with imaginary parts, while non planar diagrams imply purely real amplitudes at high energy. As an example, in Fig. 32 diagrams describing meson meson scattering and backward meson baryon scattering are illustrated. Similar duality diagrams can be drawn for processes such as meson-baryon  $\rightarrow$  meson-meson-baryon (Fig 33).

One should pay a special attention to the role of the pomeron in duality diagrams. For example  $K^+p$  and  $pp$  scatterings are controlled at high energies by the pomeron so that we cannot allow the pomeron to be dual to resonances. One possible reason for this is that its slope seems to be smaller than other trajectories. There-

fore dual models should be constructed for amplitudes from which the pomeron contribution has been removed (Collins, 1971;1972).

The duality diagrams make no reference to characteristics such as spin, and this in turn makes the duality diagrams limited.

### 3.6- DUALITY, DECK EFFECT AND THE $A_1$

Earlier in this chapter we saw that high energy Regge behaviour is consistent with low energy resonance behaviour only if extrapolation of the smooth Regge representation down to low energy gives a certain semi-local average over the resonance peaks. In other words, what is usually called the peripheral approximation to a reaction amplitude must, without containing poles in the energy plane in a rough sense, represent the resonances. Chew and Pignotti (1968) argue that the Deck peripheral model for the reaction  $\pi N \rightarrow \pi p N$  (Fig 34) explaining a peak in the final  $\pi p$  mass spectrum without explicit insertion of a resonance therein, fails to imply the absence of a resonance. On the contrary, duality means that when peripheral models predict large cross sections at low subenergies (i.e. energy of a subsystem) there probably are resonances present.

However, they observe that the concept of duality makes empty a discussion of whether there is an  $A_1$  or just an enhancement by some peripheral mechanism : Resonances are generated by peripheral exchanges. The Regge (or elementary) pion exchange amplitude is the appropriate high energy description of the  $\pi p$  system. When extended down to threshold it provides an average description of that mass region. If the smooth average is large at low mass, duality requires the existence of resonances. Some more detailed discussion will be made in the following chapter.

@@@@@@@@@@

@@@@@@

@@

## CHAPTER 4

### Further investigations and conclusion

Previously we saw a successful Deck model description of  $A_1$ -like objects would, through an extension of the duality hypothesis, support the contention that these enhancements were mainly resonant in nature. Here, we wish to study this in some more detail.

The Deck model for the reaction  $\pi N \rightarrow \pi' N$  has been given in Fig 34, corresponding to a double Regge pole representation which is valid when both of the  $\pi N$  and  $\pi' p$  final subenergies are large. Supposing that one can keep fixed all the relevant variables except the  $\pi' p$  subenergy, one gets a singly peripheral description. Now one can argue duality reasoning : If the Deck model is accurate for large values of the  $\pi' p$  subenergy, duality requires the model to yield a semilocal average description of the cross section at low values of this subenergy.

Let us assume factorization of the amplitude on its variables as either one or the other become large :

$$A(s_{\pi' p}, s_{\pi N}) \sim g_{\pi' p}(s_{\pi' p}) g_{\pi N}(s_{\pi N})$$

where Regge behaviour on each factor is assumed for, say,  $s_{\pi' p} > N_{\pi' p}$  and  $s_{\pi N} > N_{\pi N}$  :

$$\begin{aligned} g_{\pi' p}(s_{\pi' p}) &\sim c_{\pi' p} s_{\pi' p}^{\alpha_1} \\ g_{\pi N}(s_{\pi N}) &\sim c_{\pi N} s_{\pi N}^{\alpha_2} \end{aligned} \quad (4.1)$$

Keeping  $s_{\pi N}$  fixed at a value greater than  $N_{\pi N}$ , duality says that a certain average of  $g_{\pi' p}(s_{\pi' p})$  over the range  $s_{\pi' p}$  below  $N_{\pi' p}$  will be given by (4.1). The result will not be altered if we keep  $s$  rather than  $s_{\pi N}$  fixed. Now, suppose  $s$  to be sufficiently large that  $s_{\pi N}$  lies ab-

ove  $N_{\pi N}$  for all  $s_{\pi p}$  below  $N_{\pi p}$ , then

$$A(s_{\pi p}, s) \underset{s \text{ large}}{\sim} \epsilon_{\pi p}(s_{\pi p}) C_{\pi N}(s_{\pi N}(s, s_{\pi p}))^2.$$

We define the amplitude

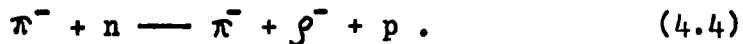
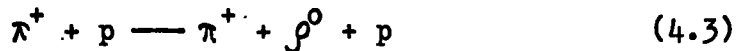
$$\bar{A}(s_{\pi p}, s) \equiv (s_{\pi N}(s, s_{\pi p}))^{-2} A(s_{\pi p}, s) \quad (4.2)$$

which exhibits the duality phenomenon when averaged over low  $s_{\pi p}$  at fixed (large)  $s$ . Since the term in brackets of (4.2) is positive definite and smoothly varying, we conclude that an average of  $A(s_{\pi p}, s)$  itself over the low  $s_{\pi p}$  region, with  $s$  fixed at a large value is correctly given by the double Regge representation. This is the desired result.

Since for singly peripheral models the prediction of large low energy cross sections corresponds to the presence of resonances, the same is likely for multiply peripheral models. Thus, Dock's calculation might be described as a prediction of the  $A_1$  !

On the other hand, however interesting the result may be, there are some objections to the above discussion. The first one is that duality relates imaginary parts of Regge exchanges to resonances, pion exchange gives primarily a real exchange amplitude. Chew and Pignotti (1968) extend the application of duality in order to make statements about  $|A|^2$  and not about  $\text{Im } A$ . This extension has little support from the very well known  $2 \rightarrow 2$  processes. Therefore, since the real part of the  $t$  channel Regge amplitude is not related by duality to the low mass  $s$  channel amplitude, there may be only a fortuitous agreement between the Reggeized Deck model and the low mass enhancements.

Another objection is due to Cohen et al (1972). They study the two reactions



They use Reggeized Deck model as a framework to compare the dual regime of (4.3) with the identical kinematic region in the 'charge exchange' reaction (4.4). In order to compare the data with the predictions of a Reggeized Deck calculation, they restrict their sample of events to the kinematic region appropriate to the model, i.e.,  $t_{\pi \rightarrow \rho\pi} < 0.5 \text{ GeV}^2$ ,  $t_{\pi \rightarrow \rho} < 0.5 \text{ GeV}^2$  and  $M_{\rho\pi} > 1.5 \text{ GeV}$ . The square of the matrix element displayed in figures 34 and 35 is

$$|M|^2 = q^2 B(s_{\pi\pi}) \frac{\beta}{1 - \cos\alpha_{\pi\pi}} (s_2/s_0)^{2\alpha_{\pi\pi}} s_1 q_1^2 \left( \frac{d^2\sigma}{dt dm} \right)_{\text{exp}}$$

where  $q$  is the momentum of the pion from the  $\rho$  decay, calculated in the rest frame of the  $\rho$ ,  $B(s_{\pi\pi})$  is a function which describes the  $\rho$  line shape;  $\alpha_{\pi\pi} = t_{\pi \rightarrow \rho} - m^2$ ;  $s_0 \approx 1 \text{ GeV}^2$ ,  $\beta$  is some constant and is the product of form factors plus couplings at the  $\rho$  vertex,  $s_1$  is the square of invariant mass of the  $\pi N$  system;  $q_1$  is the momentum of  $N$  in the  $\pi N$  rest frame;  $s_2 = s_{\pi\rho} - t_{\pi \rightarrow \rho\pi} - m^2$ ; and  $\left( \frac{d^2\sigma}{dt dm} \right)_{\text{exp}}$  is the experimentally measured on-mass shell  $\pi^+ p$  elastic scattering cross section for reaction (4.3) and the charge exchange cross section for  $\pi^- p \longrightarrow \pi^0 n$  for reaction (4.4).

The  $\rho\pi$  mass spectra for the selected events from both the reactions (4.3) and (4.4) are shown in Fig 36. It is surprising that these simple calculations provide an adequate representation of both the shape and the magnitude of the doubly charged  $A_1$  mass region in reaction (4.4) (Fig 36b). Thus the similarity of the shapes of the two figures, for these two reactions, near the  $A_1$  region leads us to

guess that this doubly charged 'particle' ( $A_1^{--}$ ) also exists in the reaction (4.4) in the same way as  $A_1^+$  exists in the reaction (4.3).

The consistency found between the Reggeized Deck calculations and the characteristics observed for low mass enhancements (e.g.  $A_1$ ) were cited as confirming evidence for the equivalence of the resonant and the Regge descriptions of these objects. However, the close agreement between the calculated and the experimental spectra for the exotic enhancement in reaction (4.4) suggests a re-examination of the 'simple' dual interpretation of the success of the Reggeized Deck model, as, otherwise, the result would show the existence of an exotic meson ( $I=2$ ).

In brief, Cohen et al conclude that one cannot use the Chew, Pignotti argument for the support of the resonant interpretation of  $A_1$  like particles, unless one also accepts the existence of exotic meson resonances. Therefore the situation of the  $A_1$  remains unclear and debates go on.

#### 4.1- A DUAL MODEL FOR THE $A_1$

Dual models present us with an opportunity to resolve the problem. Let us study the diagram in Fig 37 which is due to Berger(1971). For the case of  $A_1$  production in the reaction  $\pi p \rightarrow \pi p p$ , particles are identified in parentheses. The  $A_1$  is a threshold enhancement in the (23) system. The dual amplitude for the reaction  $ab \rightarrow 123$  should contain all known resonances present in the final state. For instance, in the (23) channel, there may be an  $A_2$  resonance as well as all recurrences of the pion. Furthermore, the amplitude will have a pion exchange pole in the  $t_{b3}$  variable which supplies the usual Deck background. Working in the dual framework has the advantage

that both Regge exchange terms and direct channel resonances appear in the amplitude in an explicitly dual manner. In principle, therefore, we have an excellent framework in which to ask whether fits to experimental distributions require an  $A_1$  resonance and/or an  $A_1$  trajectory. Note that the mere existence of dual models does not solve the problem of whether the  $A_1$  is a resonance. Only the data can decide, and so we must fit the data. Before that, we are free to construct amplitudes which have explicit  $A_1$  resonance poles as well as amplitudes which explicitly do not. However, we are not free to leave out pion exchange, since pions are known to exist. The dual framework allows us to construct amplitudes which are meant to be a proper description of pion exchange, both in the high energy region and near threshold.

Unlike the other papers on dual models for diffraction dissociation (Pokorski and Satz, 1970; Bartsch, 1970), which assume that threshold enhancements must be represented as resonance poles, Berger dispels this notion in his model. He explicitly assumes that there is no pole in the  $A_1$  region. In the diagram of Fig 37, pomeron exchange couples the upper  $\bar{p}p$  vertex to the lower dissociation one. Since we want to have no direct channel poles near the  $\pi p$  threshold, the  $A_1$  trajectory as well as the first recurrence pole of the pion trajectory is excluded.

The amplitude relevant to the figure 37 where spin dependence is ignored and which has no resonances near the  $A_1$  location is

$$A_{\pi p \rightarrow \pi p} = C s_{12}^{\alpha_p} \exp(\lambda t_{a1}) (B_4(-\alpha_{\pi}(t_{b3}), 1-\alpha_p(t_{b2})) + B_4(-\alpha_{\pi}(s_{23}), -\alpha_{\pi}(t_{b3})) + \dots) \quad (4.3)$$

where the dots stand for terms which are necessary to enforce crossing symmetry but we need not consider them here, The only term which is crucial in determining the  $\pi p$  mass distribution near threshold is the first one. The second term contributes in generating the signature factor for the exchanged pion.

In the high energy limit,  $s_{23} \rightarrow \infty$ , with  $t_{b3}$  fixed, equation (4.3) becomes

$$A_{\pi p \rightarrow \pi p} \longrightarrow C s_{12}^{\alpha_p} \exp(\lambda t_{al}) (1 + e^{-1\pi\alpha_{\pi}(t_{b3})}) s_{23}^{\alpha_{\pi}(t_{b3})} \Gamma(-\alpha_{\pi}(t_{b3})),$$

which in turn shows the correct Regge behavior associated with a doubly peripheral ( $\pi, P$ ) exchange graph. Using  $\alpha_{\pi}(t) = 0.9(t - m_{\pi}^2)$ ,  $\alpha_p(t) = 0.5 + 0.9t$  and  $\alpha_p = 1$ , the normalized cross section  $d\sigma/dM_{\pi p}$ , computed from (4.3) is given in Fig 38 which is in good agreement with data. Thus, the  $A_1$  bump can be explained perfectly well, purely as pion exchange background, even within an explicit dual framework.

As it is implied, in calculating the amplitude (4.3), several approximations have been made : Ignorance of spin dependence; the pomeron (since it is not an ordinary Regge trajectory in dual model, if it were dual to resonances, then exotic states would exist); and, of course, unitarity. Better agreement can be achieved if any of these approximations is handled.

\* \* \*

To have a nice ending we discuss the following :

A bump is observed at about 1.4 Gev in the  $\pi N$  invariant mass spectrum in  $\pi$  production experiments at high energy in  $pp \rightarrow p + (\pi N)^+$  processes and is often interpreted as a resonance. One can ask if

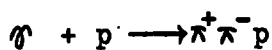
this bump is due to a resonance. Therefore, as in the case of the  $A_1$ , there are two ways of interpreting the 1.4 Gev bump; one regards the peak as a resonance with an appropriate background, and the other regards it as a kinematical effect. It is worth mentioning that a Deck type model can show the existence of the bump.

Kagiyama and Masayuki (1970) give a model (Fig 39) which is based on the Deck type model. The two other alternative figures which are equally valid are shown in figure 40. However one can show that the contributions from these two figures to  $S_1^1$  and  $P_1^1$  are of almost the same magnitude and of opposite signs. Therefore, the resultant is due to Fig 39, where, neglecting the spin dependence, the appropriate amplitude can be written as

$$T = \bar{u}(q_2) \left( \frac{1}{2} M \frac{F_\pi(\Delta^2)}{\Delta^2 + \mu^2} \sigma_{\text{tot}}^{\pi N}(\omega) g_{\pi N}^{\frac{1}{2}}(t) (\omega^4 - 2\omega^2(M^2 - \Delta^2) + (M^2 + \Delta^2)^2)^{\frac{1}{2}} \right) \cdot \gamma_5 u(p_2)$$

where  $g_{\pi N}(t)$  is the  $t$  dependence factor of the differential cross section ( $d\sigma/dt^2 = A \exp(-bt^2)$ ) and  $F_\pi(\Delta^2)$  is the form factor of the off mass shell pion and is normalized to  $3^{\frac{1}{2}}g$  at  $\Delta^2 = -\mu^2$ ,  $g^2/4\pi = 14.7$ .

To support the idea of a major part of the bump having a kinematical nature, one can say that this bump has not been seen in the photo- or electron-pion production, such as



at high energy. Besides, if we have a process where the Deck mechanism does not work, the 1.4 Gev bump will disappear. The  $\pi^- p$  invariant mass in  $\pi^- p \longrightarrow \pi^0 \pi^- p$  may be such an example. In this process the backward scattering of  $\pi^0 \pi^-$  at high energy works but not the diffrac-

tion scattering. If the backward scattering of  $\pi^0 \pi^-$  is dominated by a  $\rho$  Regge pole and the backward differential cross section is proportional to the factor  $\exp(-Bt^2)$ , where  $t$  is the four momentum transfer from the outgoing  $\pi^0$  to the incident  $\pi^-$ , there is also some kinematic constraints on the distribution of the final particles. Thus, the bump is neither the pure resonance nor the average of some resonances but the kinematical effect due to the diffraction scattering at least for its major part.

On the other hand, if the Chew-Pignotti line of reasoning holds true, the dissociated system will be controlled by the  $\pi$  Regge pole. Two invariant mass spectra are different: the  $\pi^+ n$  combination has the 1.4 Gev bump but the  $\pi^- p$  combination does not. The difference between the two combinations comes from the difference of the Regge pole exchange between the incident  $\pi^-(\pi^+)$  and the dissociated  $\pi^0(\pi^+)$  so that this means that the 1.4 Gev bump is generated mainly by the interaction between one of the dissociated particles and the other initial particle, that is, the bump is almost the kinematical effect.

\* \* \*

#### 4.3- SUMMARY AND CONCLUSION

As we saw in chapter two, the  $A_1$  appears as an enhancement just above  $\pi\rho$  threshold. For some time, it was thought that the  $A_1$  was a weak resonance supported by a large kinematic (Deck) background. This interpretation is difficult because both 'resonance' and background appear to have  $J^P=1^+$ . On the other hand, the full width of the  $\pi\rho$  mass distribution generated in the simple Deck model is not as narrow as that of peaks observed experimen-



## REFERENCES

- ABBBHL Collaboration (1965). Phys. Rev. 138, B897.
- Abolins et al (1966). Phys. Lett. 21, 584.
- Alessandrini, Amati, Squires (1968). Phys. Lett. 27B, 463.
- Anderson et al (1969). Phys. Rev. Lett. 22, 1390.
- 
- Barry (1967). Leçon sur la théorie des groupes et les particules élémentaires.
- Barger, Cline (1967). Phys. Rev. 155, 1792.
- Bartsch et al (1970). Nuc. Phys. B24, 221.
- Bellini et al (1963). Nuo. Cim. 29, 896.
- Berger (1968). Phys. Rev. 166, 1525.
- Berger (1971). Caltech Conf. on Particle Phen., 167.
- Bernstein (1968). Elementary particles and their currents.
- 
- Calucci, Ghirardi (1968). Phys. Rev. 169, 1339.
- Carruthers (1966). Introduction to unitary symmetry.
- Chew (1966). Lawrence Rad. Lab., California, UCRL -16983.
- Chew, Pignotti (1968). Phys. Rev. Lett. 20, 1078.
- Chung et al (1964). Phys. Rev. Lett. 12, 621.
- Cohen et al (1972). Phys. Rev. Lett. 28, 1601.
- Collins (1971). Phys. Reports 1C, No 4, 181.
- Collins (1972). British Univ. Summer School, 58.
- Collins, Johnson, Squires (1968). Phys. Lett. 27B, 23.
- Palitz (1973). *Invited paper presented at Smolenice, Czechoslovakia.*
- Dalitz, Moorhouse (1970). Proc. Roy. Soc. 318, 279.
- Deck (1964). Phys. Rev. Lett. 13, 148.
- Deutschmann et al (1966). Phys. Lett. 22, 112.
- Diebold (1972). Proc. XVI Inter. Conf., Batavia.
- Dolen, Horn, Schmid (1967). Phys. Rev. Lett. 19, 402.
- Dolen, Horn, Schmid (1968). Phys. Rev. 166, 1768.
- Donnachie (1970) Proc. Roy. Soc. 318, 307.
- 
- Fox, Hey (1973). CALT-68-373.
- French (1968). Proc. Vienna Conf., 92.

Goldhaber et al	(1964). Phys. Rev. Lett. 12, 336.
Greenberg	(1969). Proc. Lund Inter. Conf., 385.
Grennell et al	(1970). Phys. Rev. Lett. 24, 781.
Harari	(1969). Phys. Rev. Lett. 22, 562.
Harari	(1970). Proc. Roy. Soc. 318, 355.
Hendry	(1965). Rutherford Preprint.
Hughes	(1972). Elementary particles.
Jackson	(1969). Proc. Lund Inter. Conf., 63.
Jackson	(1970). Rev. Mod. Phys. 42, 12.
Jacob	(1969). Proc. Lund Inter. Conf., 127.
Kagiyama, Uehara	(1970). Prop. Theo. Phys. 43, 425.
Lamsa et al	(1968). Phys. Rev. 166, 1395.
Lipkin	(1969). Proc. Lund Inter. Conf., 53.
Lipkin	(1970). Quark models for pedestrians.
Maor, O'Halloran	(1965). Phys. Lett. 15, 281.
Martin, Spearman	(1970). Elementary particle theory.
Michael	(1966). Phys. Lett. 21, 93.
Morpurgo	(1968). Vienna Inter. Conf.
Nasrollah	(1970). Nuc. Phys. B19, 167.
Phillips, Ringland	(1970). Proc. Roy. Soc. 318, 299.
Pokorski, Satz	(1970). Nuc. Phys. B19, 113.
Rabin et al	(1970). Phys. Rev. Lett. 24, 925.
Roberts	(1971). Phys. Lett. 35B, 525.
Rosenfeld	(1965). Oxford Inter. Conf.
Rosner	(1969). Phys. Rev. Lett. 22, 689.
Schmid	(1968). Phys. Rev. Lett. 20, 689.
Schmid	(1969). Nuo. Cim. 61A, 289.
Schmid	(1970). Proc. Roy. Soc. 318, 257.

Taylor

(1972). Scattering theory.

Titchmarsh

(1939). The theory of functions.

Veneziano

(1968). Nuo. Cim. 57A, 190.


.

FIGURE    CAPTIONS

- Fig 1. Dalitz plot for  $\pi^+ p \rightarrow \pi^+ \rho^0 p$  at 8 Gev/c, showing enhancement at large  $\pi\rho$  mass, including the  $A_1$  and  $A_2$  bands.
- Fig 2. A triangle Dalitz plot for  $K^+ p \rightarrow K^+ p \pi^+ \pi^-$  for 10 Gev/c kaons. The  $K^*(890)$  and  $\Delta^{++}(1236)$  resonances are obvious.
- Fig 3. An Argand diagram which exhibits all of the parameters of the relevant text.
- Fig 4. Typical resonance configurations; (a) pure Breit-Wigner,  $\Gamma^{el} \rangle \frac{1}{2} \Gamma^{tot}$ ; (b) pure Breit-Wigner,  $\Gamma^{el} \langle \frac{1}{2} \Gamma^{tot}$ ; (c) Breit-Wigner with attractive background; (d) Breit-Wigner with repulsive background.
- Fig 5. The circle of convergence of the Breit-Wigner expansion.
- Fig 6. Unphysical sheet pole lying on the real s-axis below the lowest threshold.
- Fig 7. SU(3) classification of particles (Bacry, 1967). It is interesting to see that in the meson case particles and antiparticles appear in the same multiplet whereas this is not true for baryons.
- Fig 8. Forward and backward peaks in  $\pi^+ p \rightarrow K^+ \Sigma^+$ . Here one can have either a non exotic meson or a non exotic baryon.
- Fig 9. Purely forward peak in  $K^- p \rightarrow \bar{K}^0 N$ .
- Fig 10. Purely backward peak in  $\pi^- p \rightarrow K^+ \Sigma^-$ .
- Fig 11. Scatter plots of the effective mass distribution for the two particles composite in  $\pi^+ p \rightarrow \pi^+ p \pi^- \pi^+$ . The mass projections are also shown.
- Fig 12. The projection of events on the  $M^2(\rho^0 \pi^+)$  in the reaction  $\pi^+ p \rightarrow \rho^0 \pi^+ p$  when  $N^{*++}$  is excluded.
- Fig 13. The  $\rho\pi$  enhancement.
- Fig 14. The effective mass distribution for  $\pi^+ \pi^- \pi^-$  combinations for events with  $M(\pi^+ p)$  outside the  $N^{*++}$  interval. The smooth curves represent  $3\pi$  phase space normalized to events outside the peaks.
- Fig 15. Single particle exchange diagram giving rise to a kinematical peak in the  $\pi\rho$  mass spectrum (the Deck effect).
- Fig 16. Plot of the differential cross section obtained from the diagram of Fig 15.
- Fig 17. Comparison of data of Goldhaber et al (1964) and calculated Deck diagram in  $A_1$  region.
- Fig 18. Improved Deck-type calculated curve of Maor and O'Halloran.

- Fig 19. A more realistic diagram proposed to explain the  $A_1$ .
- Fig 20. Three pion effective mass distribution for reaction  $\pi^+ p \rightarrow \pi^+ \pi^- \pi^+ p$  with both  $p\pi^+$  mass outside the  $N^*$  region (1.12 to 1.32 Gev). The curve shows the one pion exchange prediction.
- Fig 21. A resonance fit to  $\pi^+ p \rightarrow p\pi^+\rho^0 \rightarrow p\pi^+\pi^-\pi^+$  at 8 Gev/c.
- Fig 22. Reggeized Deck diagram.
- Fig 23. Comparison of Deck- and Berger-type model for the reaction  $\pi N \rightarrow \pi \rho N$  at two different incident energies.
- Fig 24. Production of  $A_1$  in the reaction  $\pi^- p \rightarrow p\pi^+\pi^+\pi^-\pi^-\pi^-$ .
- Fig 25. Missing mass spectrum plotted versus  $M^2$  for the reaction  $\pi^- p \rightarrow pB^-$  for  $M_{B^-} \ll 1.88$  Gev at an incident momenta of 16 Gev/c.  $B^-$  denotes the missing mass meson with negative charge.
- Fig 26. Three pion effective mass distribution with events in the  $\Delta^{++}$  (1238) region removed.
- Fig 27. Cross section for  $A_1^-$  and  $A_2^-$  production as a function of  $p_{lab}$ . The lines correspond to an energy dependence given by a trajectory with  $\alpha(0)=0.55$ .
- Fig 28. The descriptions of the hadronic scattering amplitude in (a) s-channel, (b) t-channel.
- Fig 29. A diagram showing the interference model.
- Fig 30. The Veneziano amplitude in the s-t plane. The poles occur where  $\alpha(s)$  and  $\alpha(t)$  pass through positive integers, and the lines of zeros connect the pole intersections diagonally in order to prevent there being double poles.
- Fig 31. Regge exchange diagram and the duality diagram for, (a)  $\pi^- p \rightarrow K^0 \Delta$  (backward), (b)  $K^- n \rightarrow \pi^- \Delta$  (forward). (a) is a planar duality diagram, while (b) is a non planar one.
- Fig 32. Diagrams for, (a) meson-meson scattering, (b) forward meson-baryon scattering, (c) backward meson-baryon scattering. The s and t channel intermediate states are marked by dashed lines.
- Fig 33. (a) Diagram for  $MB \rightarrow MMB$  and, (b) - (f) its various alternative descriptions. Every one of the five descriptions (b) to (f) may, in principle, be a complete picture of the amplitude. They should be summed over all possible intermediate states ( $B_1, B_2, M_1, M_2, M_3$ ), which are marked by dashed lines in (a).
- Fig 34. A diagram representing the Deck doubly peripheral model for the reaction  $\pi p \rightarrow \pi \rho p$ .

Fig 35. The exchange diagram for  $\pi^- n \rightarrow \pi^- \rho^- p$ .

Fig 36. Invariant mass distributions for those  $\pi \rho$  events fitted by the model described in the text.

Fig 37. A diagram illustrating diffraction dissociation of hadron b into system (23). Symbol P denotes pomeron exchange.

Fig 38. The histogram of the cross section versus invariant mass of  $\pi^- \rho^0$  from the reaction  $\pi^- p \rightarrow \pi^- \rho^0 p$  at 20 Gev/c. The solid curve is obtained from a dual model which, as described in the text, has no resonance poles in the  $A_1$  region.

Fig 39. The dominant diagram for the diffraction dissociation model.

Fig 40. The other two possible diagrams for the diffraction dissociation model similar to that of Fig 37.

\*!\*!\*!\*!\*!

@@@@@@

\*\*\*



Table 1

Particle	Quark Combination
$\pi^+$	$\bar{n}p$
$\pi^0$	$\frac{1}{\sqrt{2}}(\bar{p}p - \bar{n}n)$
$\pi^-$	$\bar{p}n$
$K^+$	$\bar{\Delta}p$
$K^0$	$\bar{\Lambda}n$
$K^-$	$\bar{p}\Delta$
$\bar{K}^0$	$\bar{n}\Delta$
$\eta^0$	$\frac{1}{\sqrt{6}}(\bar{p}p + \bar{n}n - 2\bar{\Delta}\Delta)$
$\phi$	$\Lambda\bar{\Lambda}$

From Bernstein (1968) and Lipkin (1970)

Table 2

Channel	Final State	Branching Ratio (%)	Cross Section (mb)
1a	$\rho^0 N^{*++}$	30.5	$1.17 \pm 0.12$
1b	$\rho^0 \pi^+ p$	23.0	$0.86 \pm 0.09$
1c	$\pi^+ \pi^- N^{*++}$	30.1	$1.16 \pm 0.12$
1d	$f^0 N^{*++}$	3.4	$0.13 \pm 0.04$
1e	$\pi^+ \pi^- \pi^+ p$ (non resonant)	13.0	$0.53 \pm 0.1$
	Total	100.0	$3.85 \pm 0.30$

Partial cross sections for channels leading to  $\rho^0$ ,  $f^0$  and  $N^{*++}$  (1238) formation in the reaction  $\pi^+ p \rightarrow \pi^+ \pi^- \pi^+ p$  at 3.65 Mev/c.

Table 3

Isospin	$A_1(1^+)$ Nonet
$I = 1$	$A_1(1070)$
$I = 1/2$	$Q_{A_1} = C(?)$ (1240 $\rightarrow$ 1290)
$I = 0$	$D(1285)$ $D' = E(1422)?$ or $M(953)?$

Table 4

Particle	Mass GeV/c	Decay	Width MeV/c
$A_1$	1.07	$\pi\rho$	140
$\rho_{A_1} = C$	1.24	$\pi K^*$	50
$D(1285)$	1.285	$2\pi\pi$ $K\bar{K}\pi$	$\Gamma_{ht} = 21 \pm 10$
$D' = E(?)$	1.422	$\bar{K}K^* + K\bar{K}^*$	50
$D'(\text{singlet})$	any	$\bar{K}K^* + K\bar{K}^*$	0

Table

5

A<sub>1</sub> Nonet Cross sections

Reaction	Decay	P <sub>lab</sub>	σ (μb)	
			Theory	Exp.
$\pi^+ n \rightarrow D^0 p$	$\pi_N(980)^{\mp} \pi^{\pm}$	2.7	52	44 ± 8
$\pi^- p \rightarrow D^0 n$	$K^{\pm} K^0 \pi^{\mp}$	2.5 → 2.63	Unknown D → K $\bar{K}$ n	7 ± 2
$\pi^- p \rightarrow D^0 n$	$K^{\pm} K^0 \pi^{\mp}$	2.9 → 3.3	Branching ratio	10 ± 4
$\pi^- p \rightarrow D^0 n$	$K^{\pm} K^0 \pi^{\mp}$	3.8 → 4.2		17 ± 5
$\pi^+ p \rightarrow D^+ \Delta^{++}$	$\pi^+ \pi^- \eta$	8	7	25 ± 8
$K^- p \rightarrow D^0 \Lambda$	$\pi_N(980)^{\mp} \pi^{\pm}$	5.5	1.5	< 6
$\pi^- p \rightarrow Q \Lambda$	$(K\pi\pi)^0$	4.5	8	13.5
$\pi^- p \rightarrow Q \Lambda$	$(K\pi\pi)^0$	6	6.5	8.7

# Table 6

The two descriptions of the hadronic scattering amplitude.

Approximation	Complete Description	Neglected
resonance saturation.	i) fixed $t$ -dispersion relation. ii) partial wave expansion.	non-resonating background.
Regge pole dominance.	Regge expansion	cuts, background integral

Fig 1

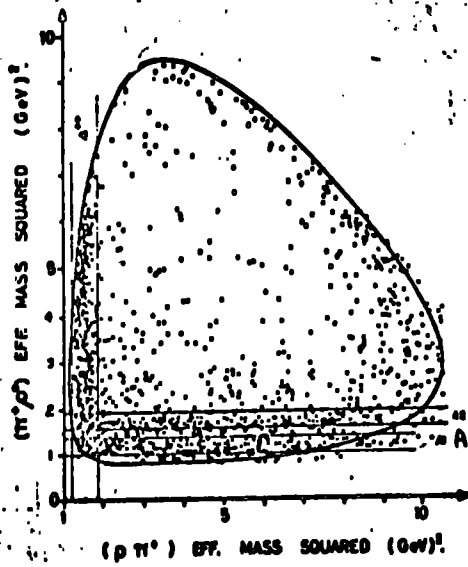
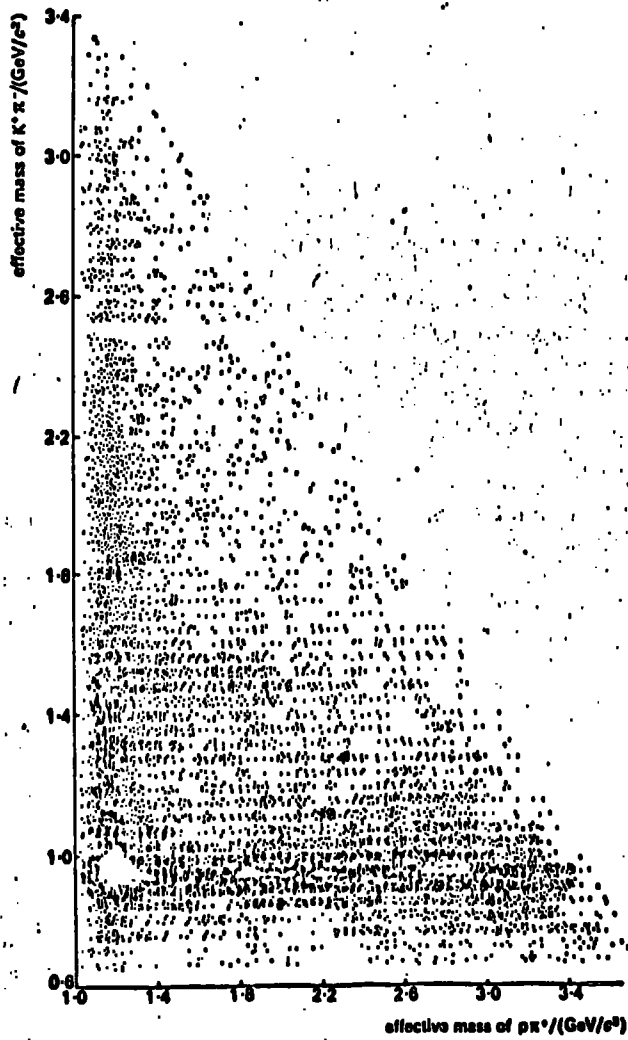


Fig 2



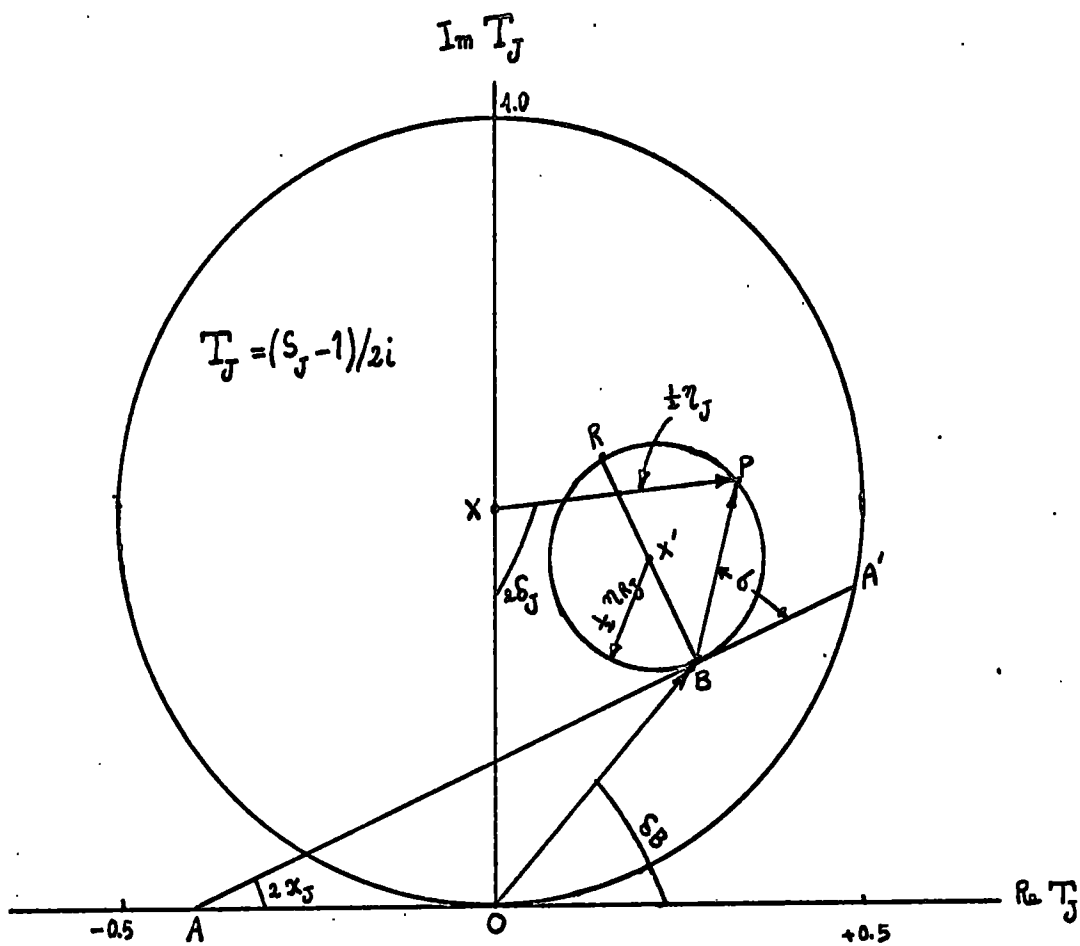


Fig 3



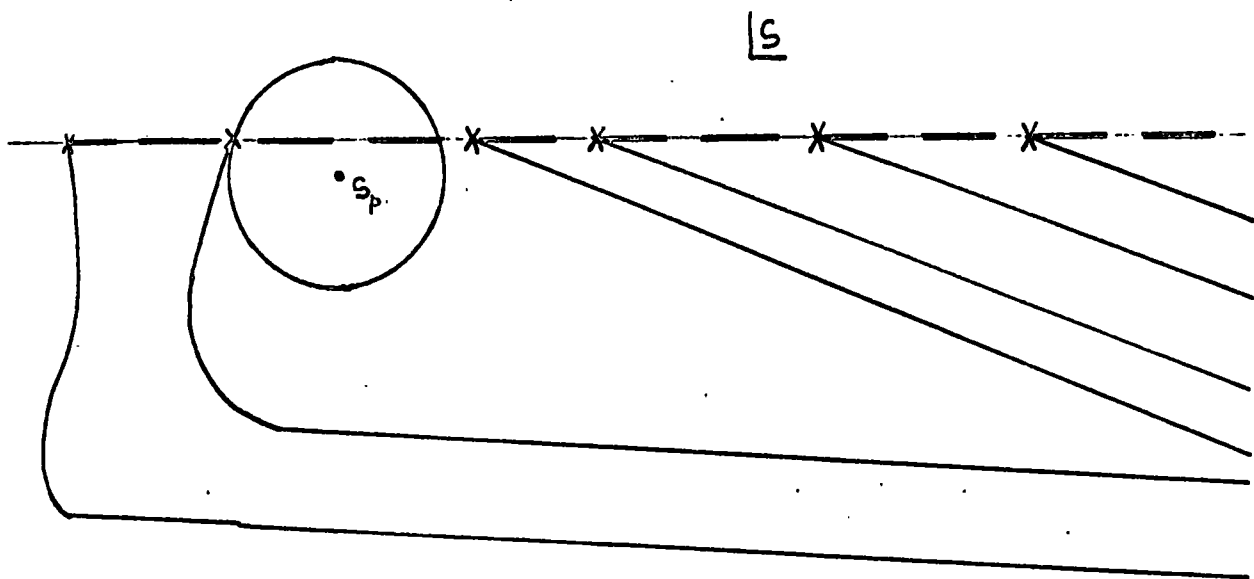


Fig 5

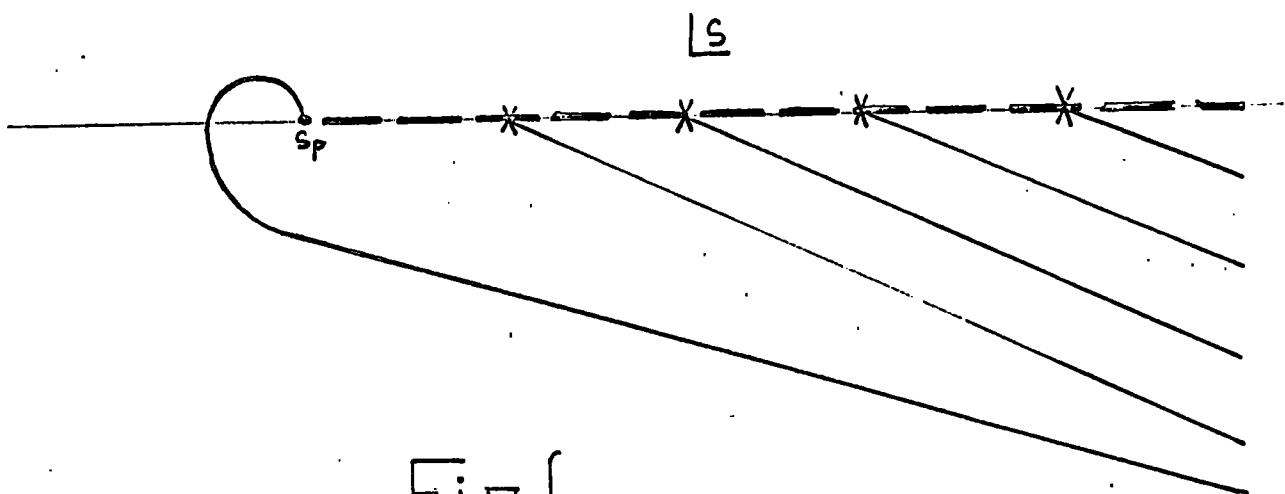
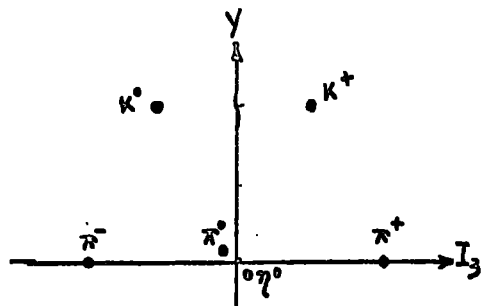


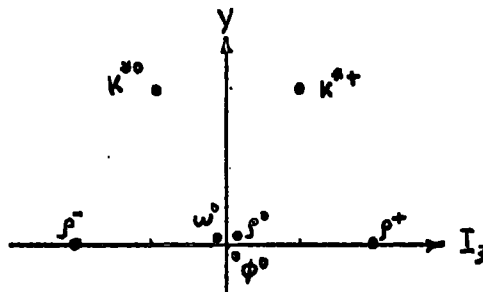
Fig 6



Pseudo Mesons Octet

$$J^P = 0^-$$

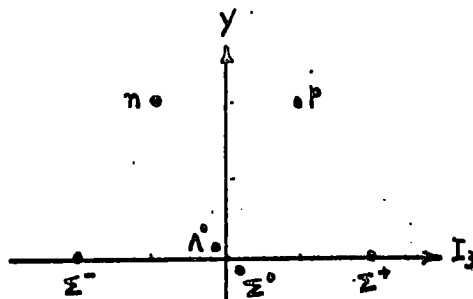
$$B = 0$$



Vectorial Mesons Nonet

$$J^P = 1^-$$

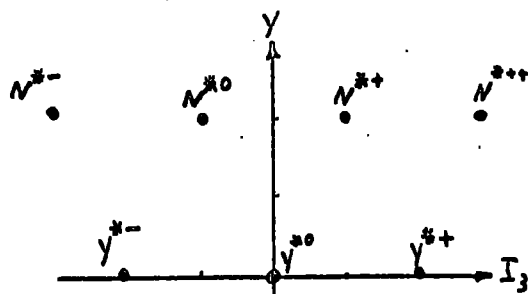
$$B = 0$$



Baryons Octet

$$J^P = \frac{1}{2}^+$$

$$B = 1$$



Baryons Decuplet

$$J^P = \frac{3}{2}^+$$

$$B = 1$$

Fig 7

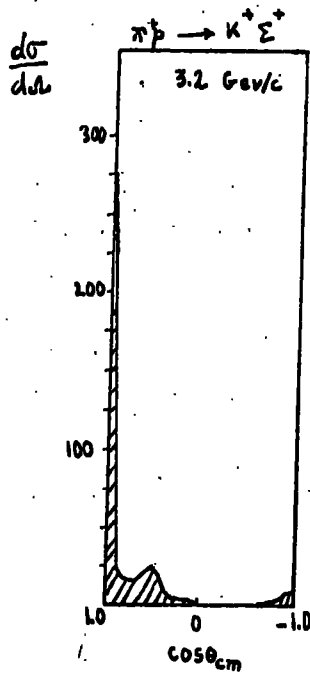
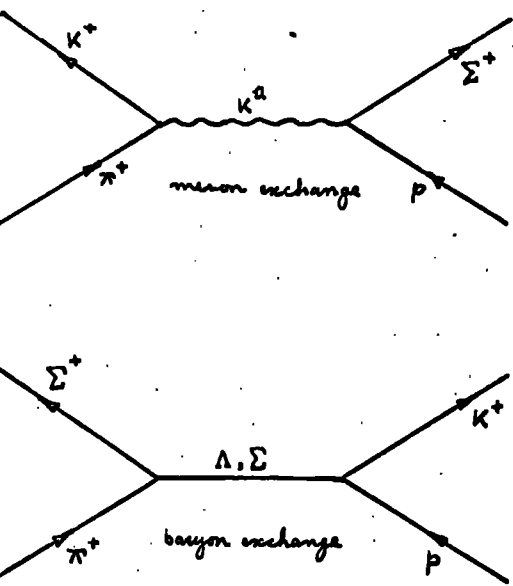


Fig 8

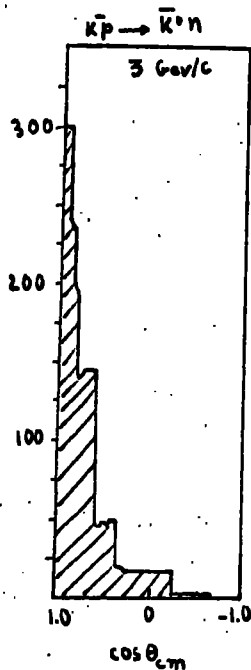
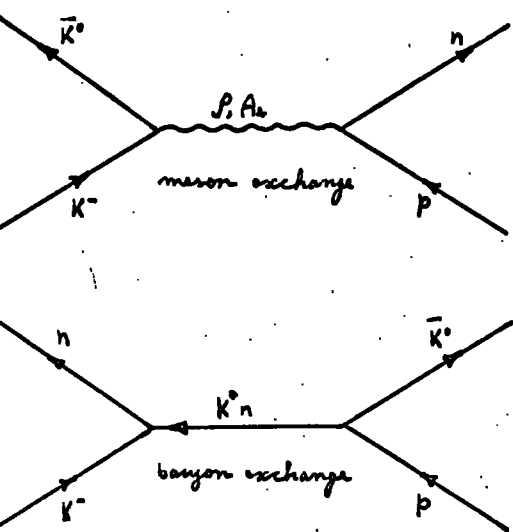


Fig 9

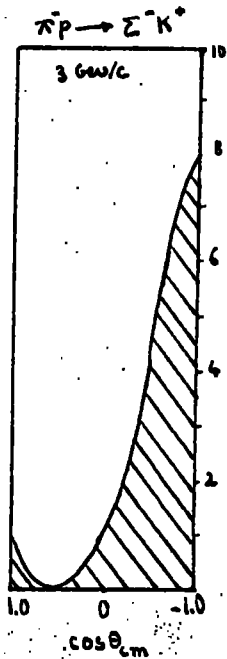
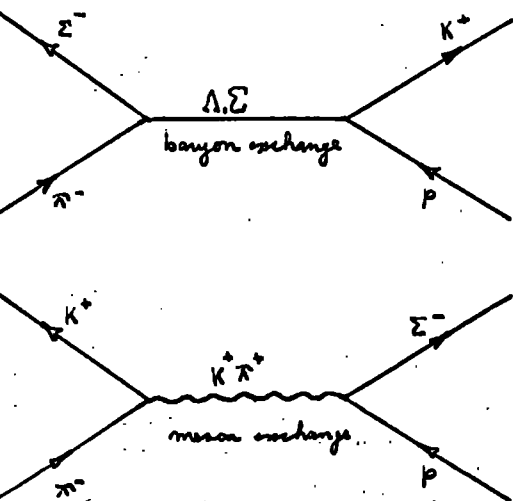


Fig 10

Fig 11

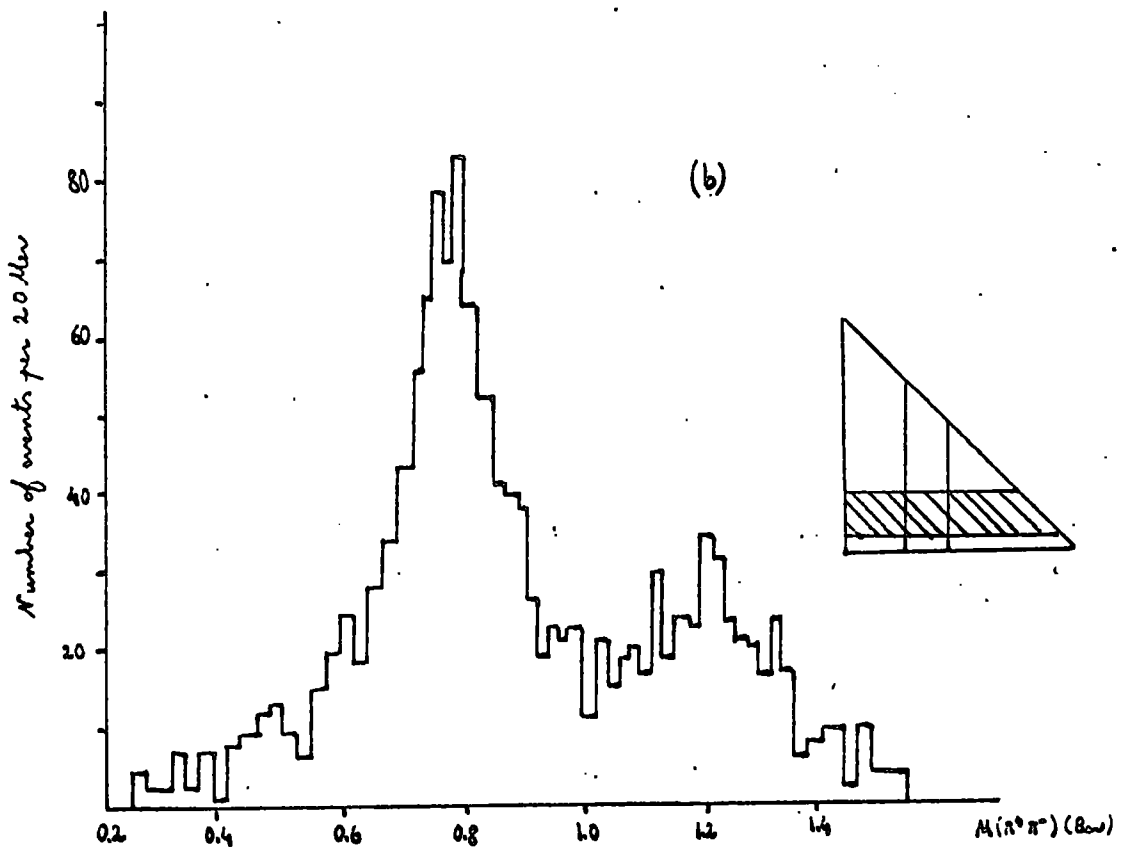
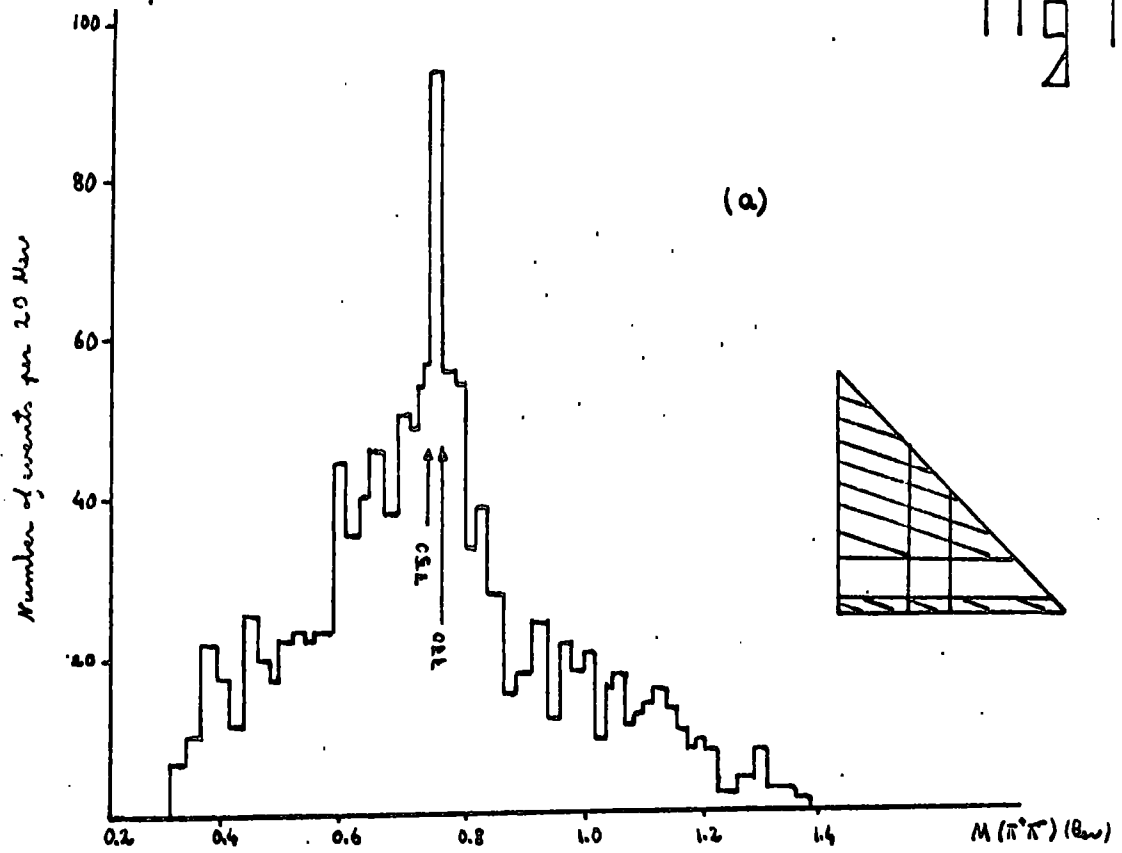


Fig 12

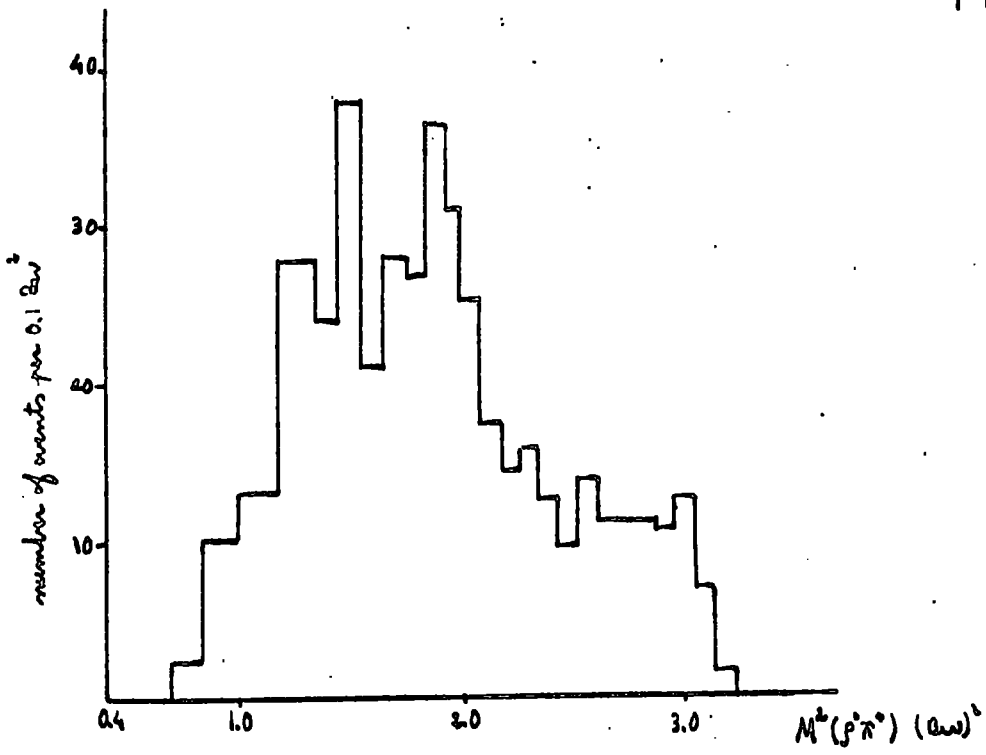


Fig 13

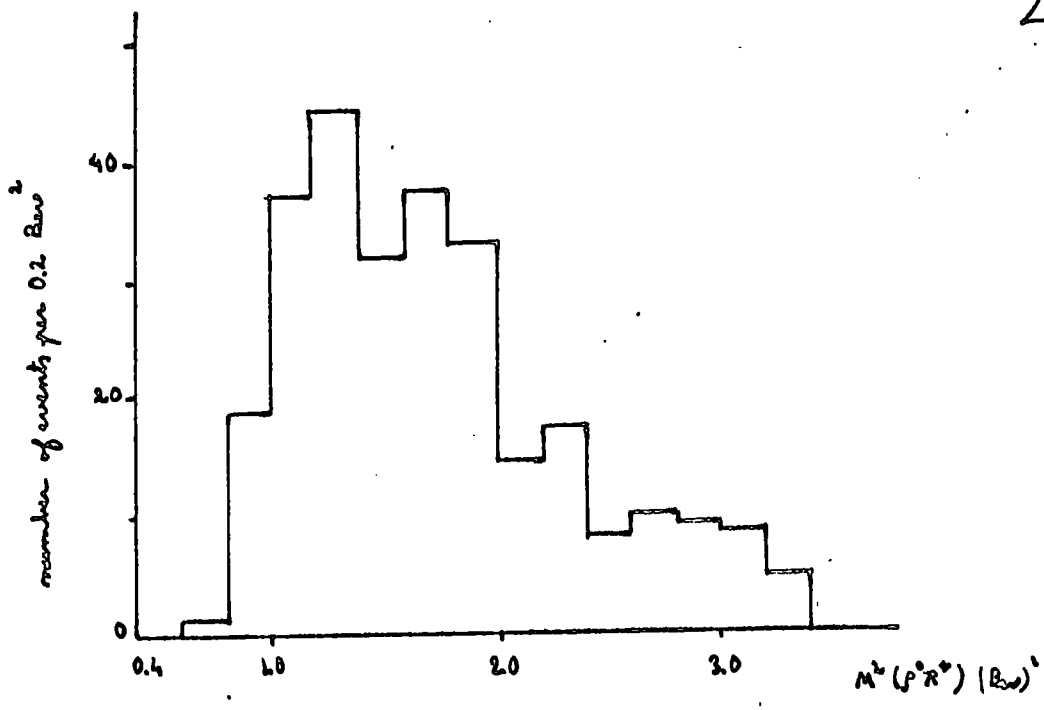
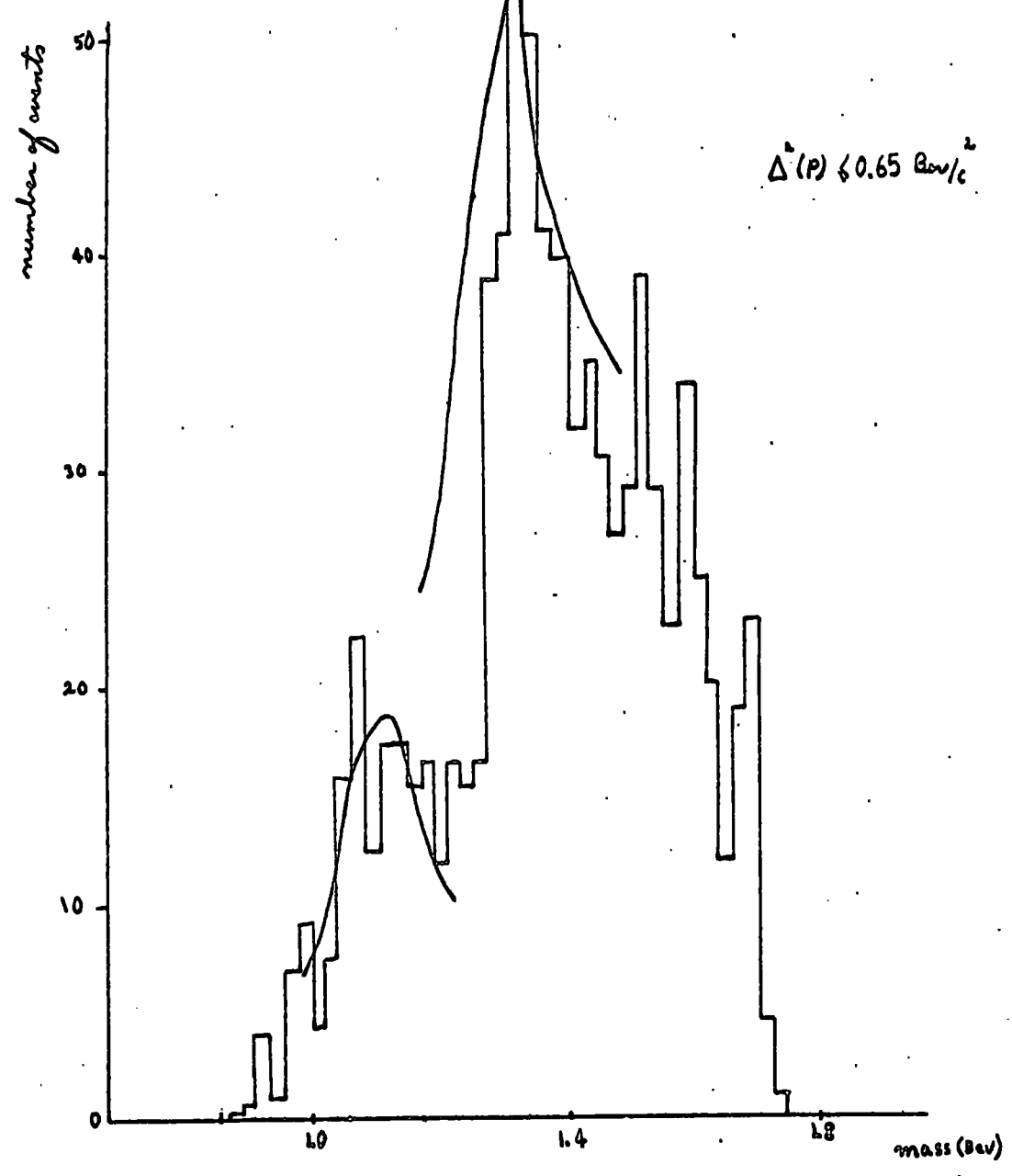


Fig 14



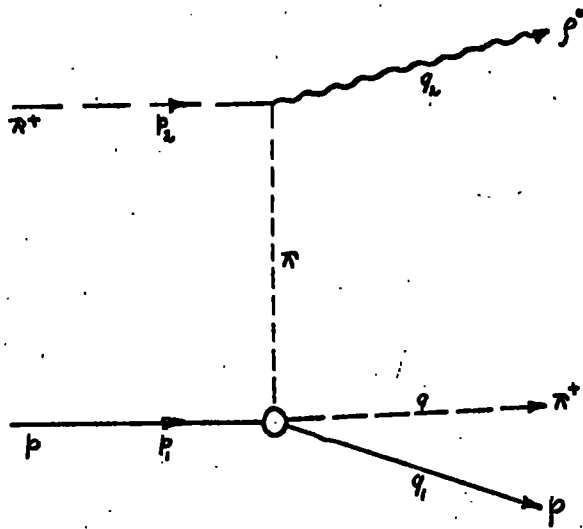


Fig 15

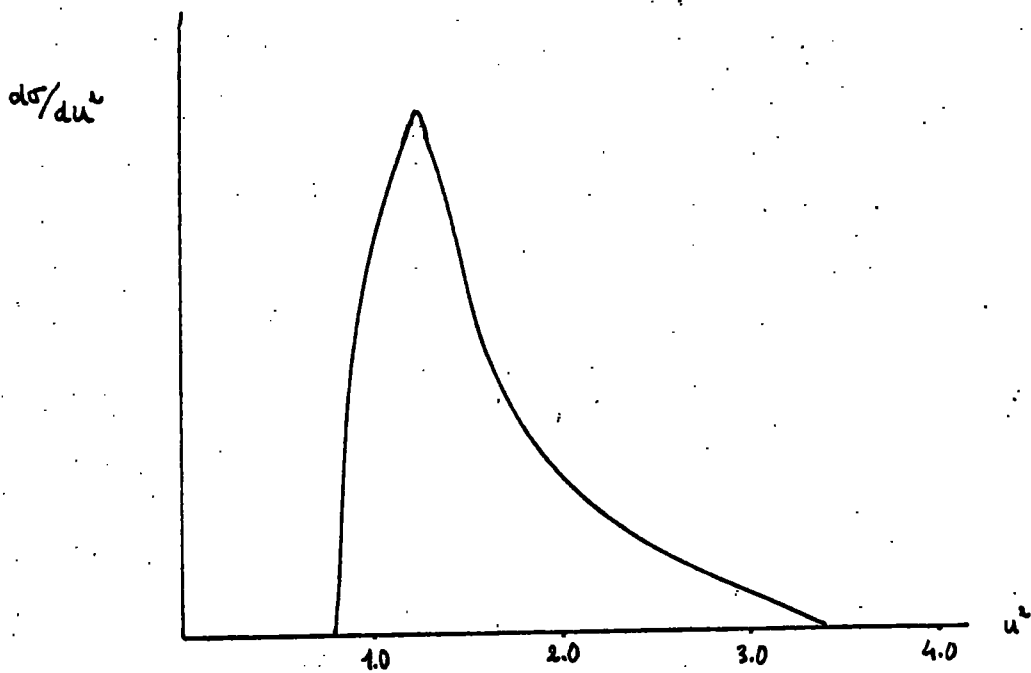


Fig 16

Fig 17

$d\sigma/du^2$

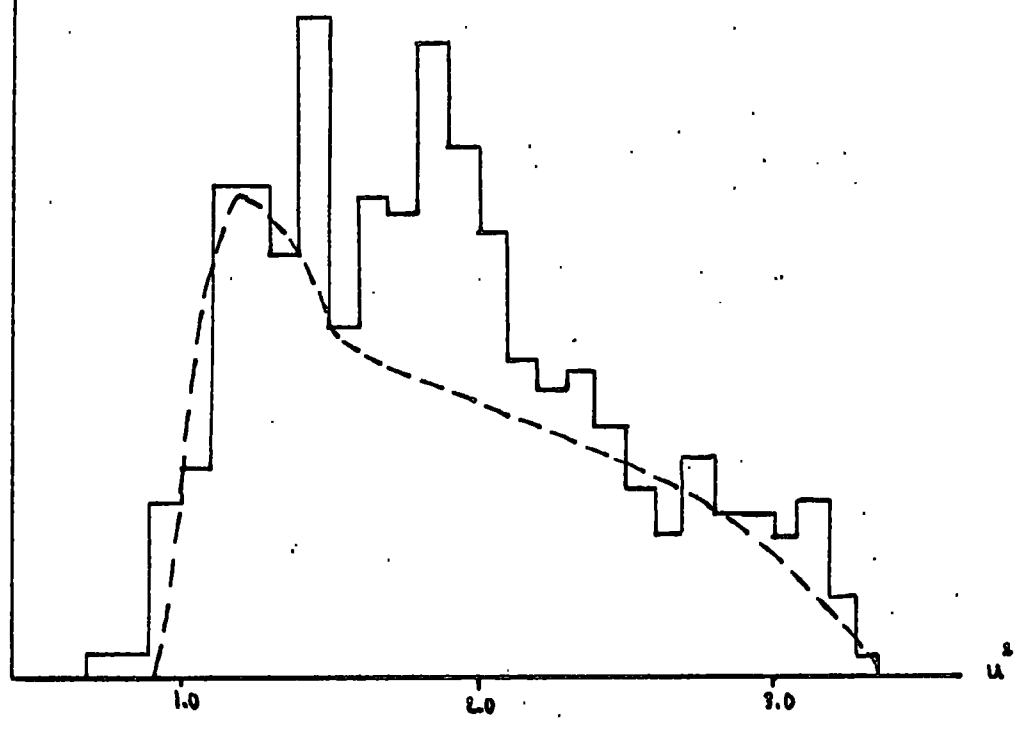
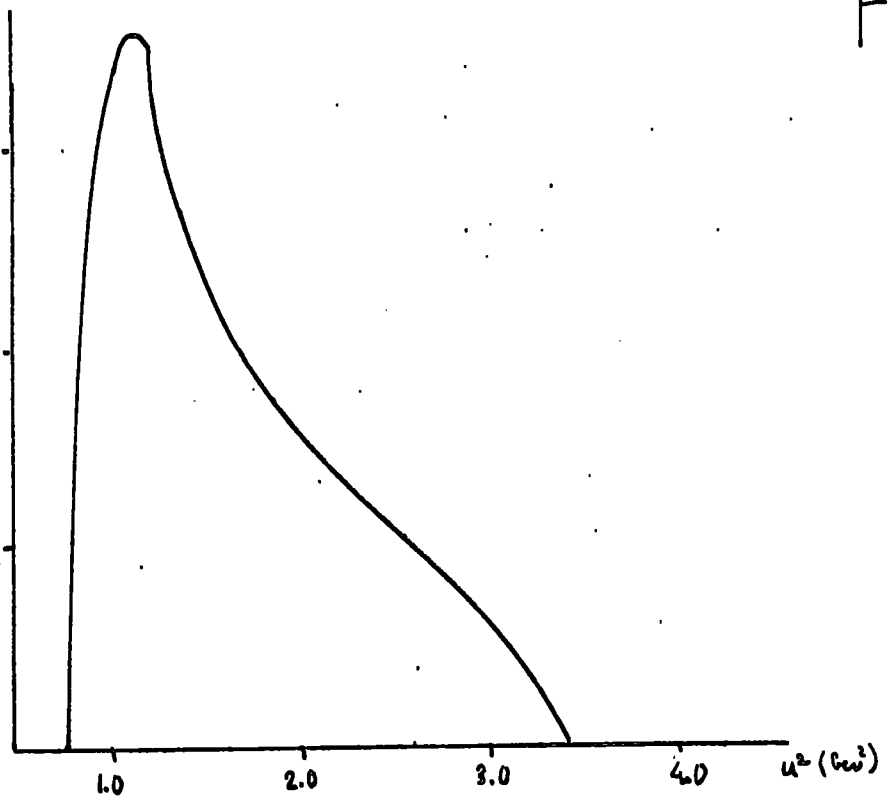


Fig 18

$d\sigma/du^2$   
(mb/cw)

0.15  
0.10  
0.05



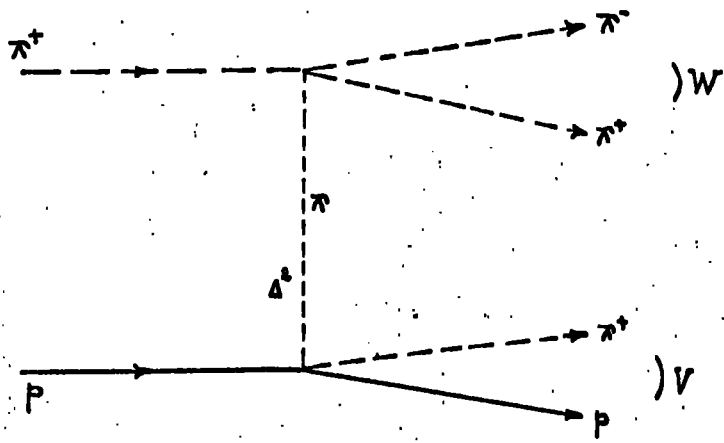


Fig 19

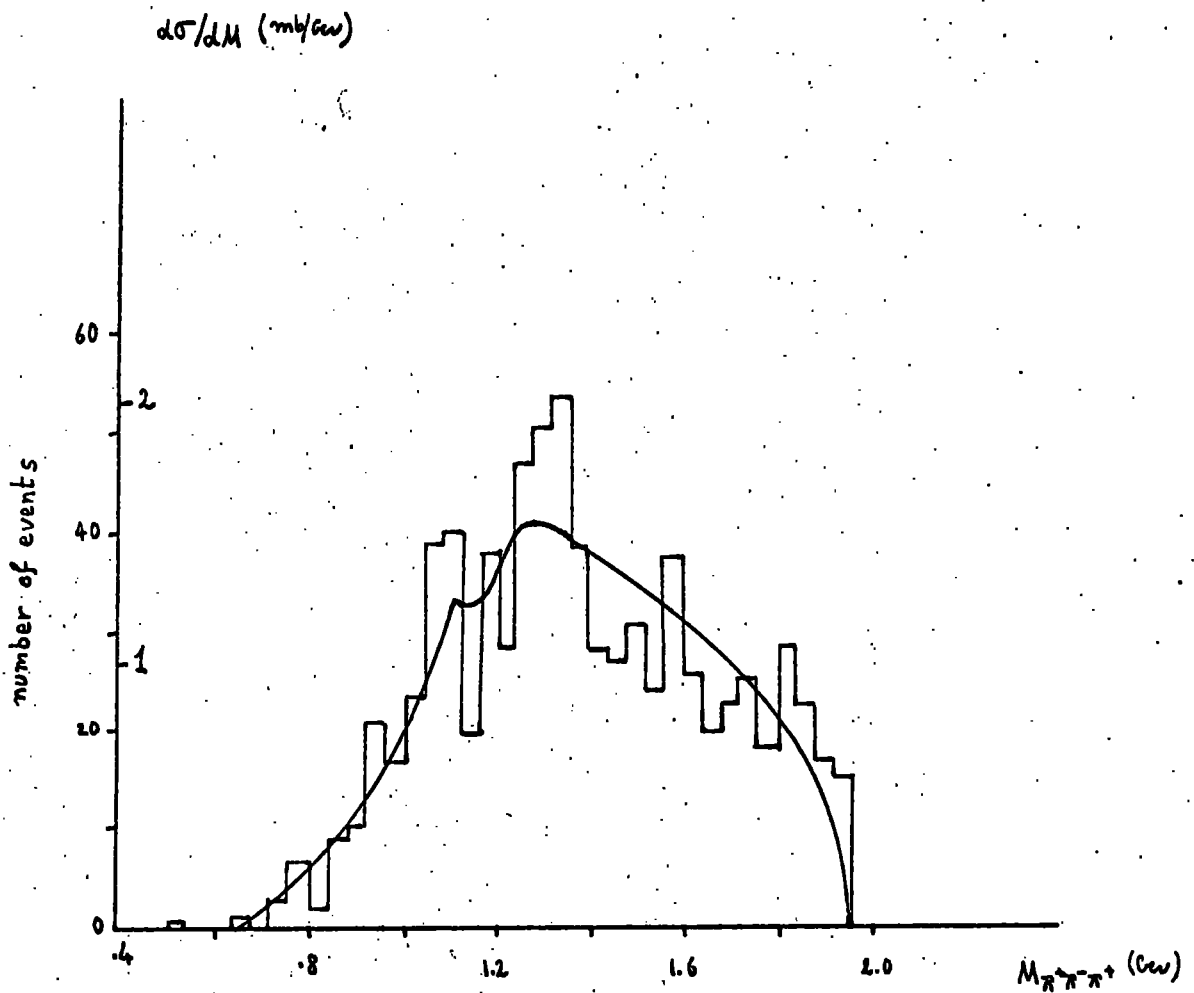
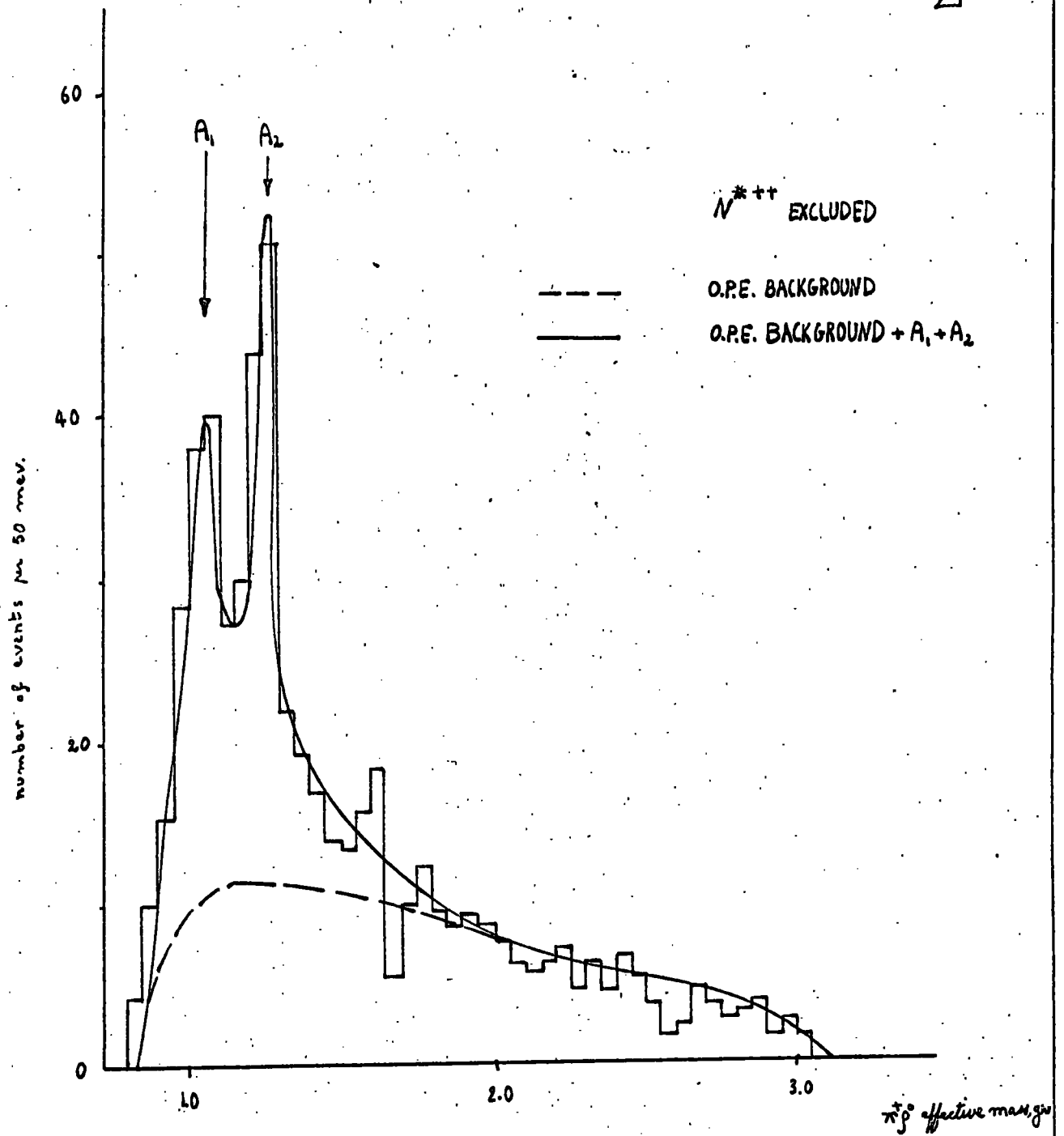


Fig 20

Fig 21



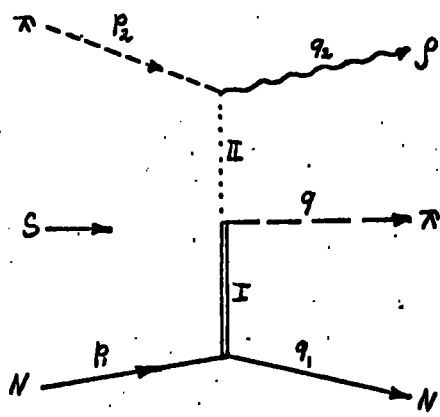


Fig 22

$dS/dW$  (mb/Bev/c<sup>2</sup>)

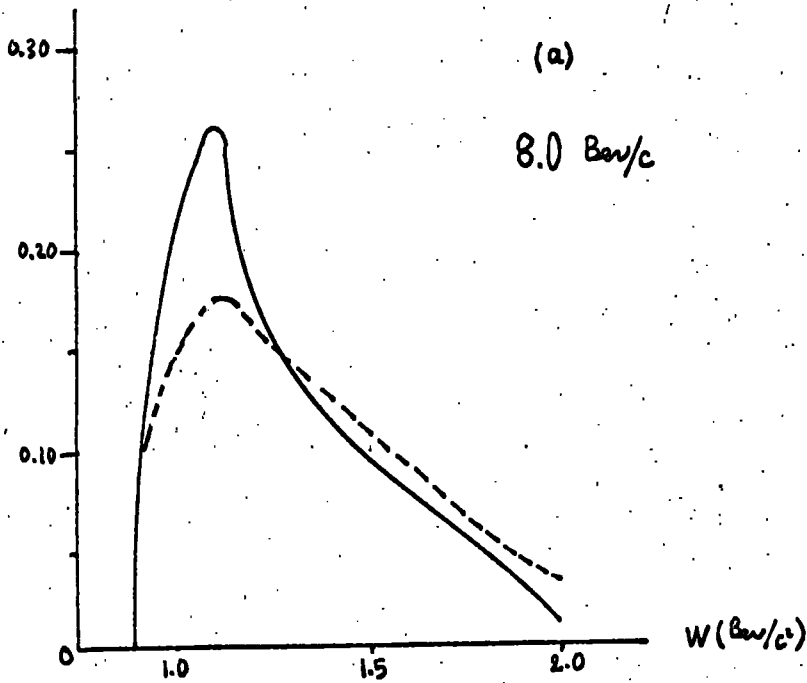
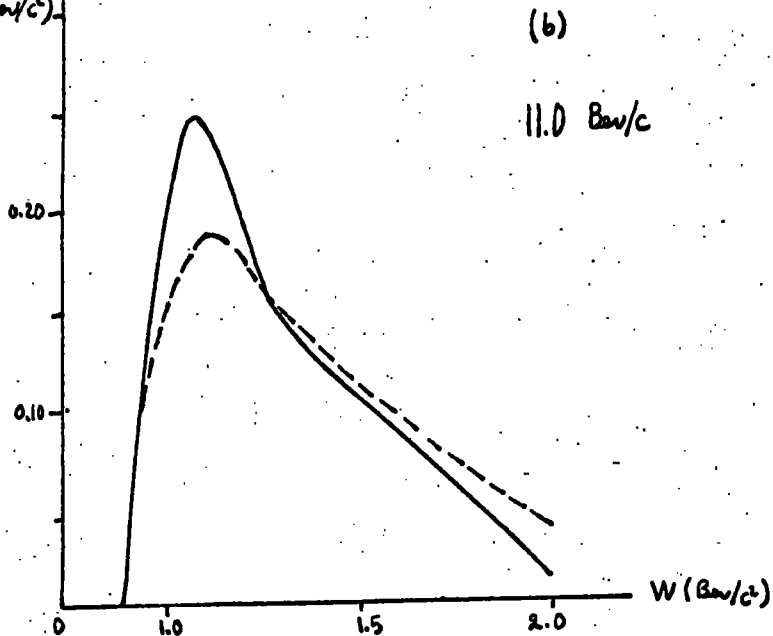


Fig 23

$dS/dW$   
(mb/Bev/c<sup>2</sup>)



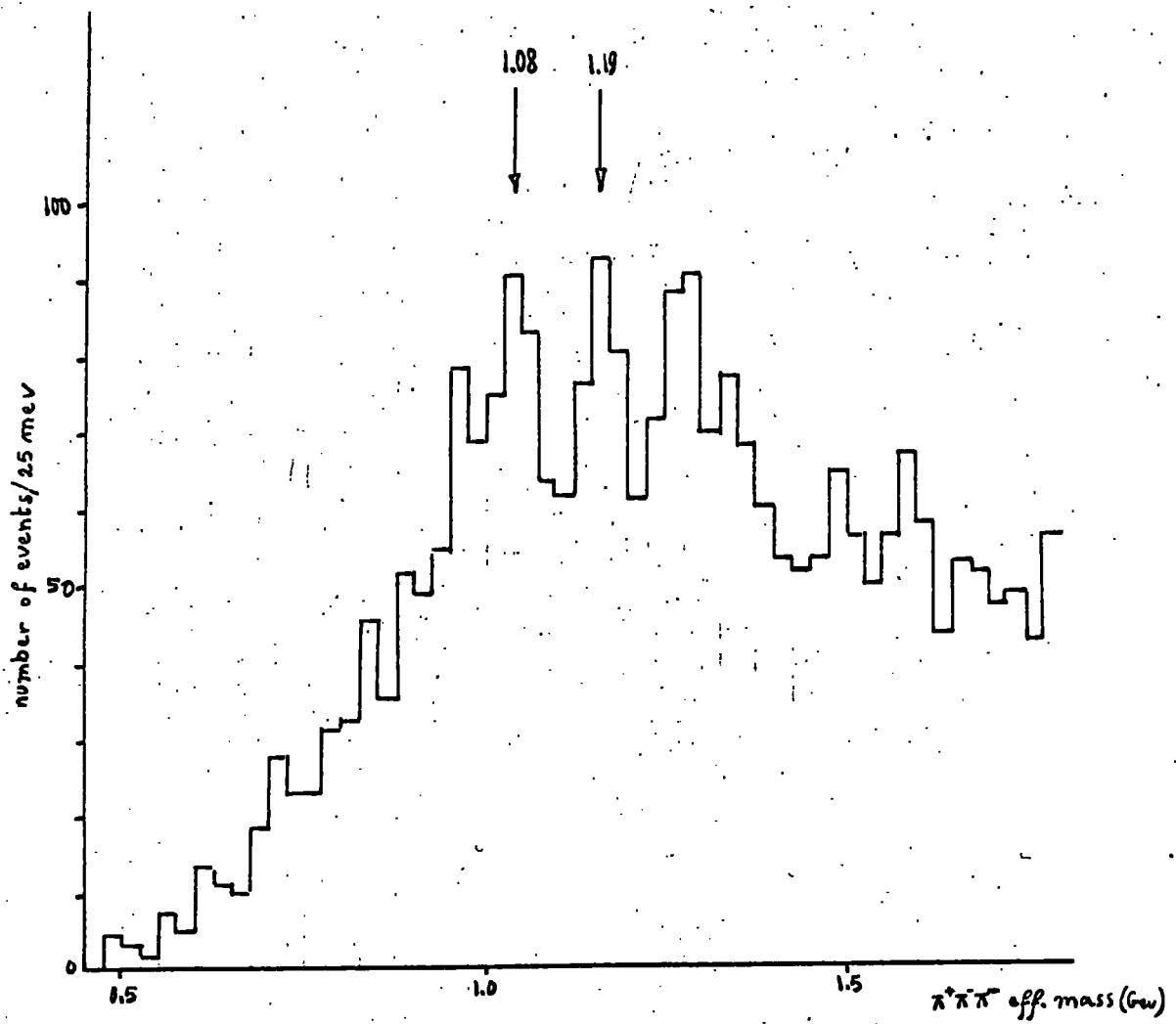


Fig 2.4

$d^2\sigma/dM^2d\Omega$   
(mb/GeV<sup>2</sup>-sr)

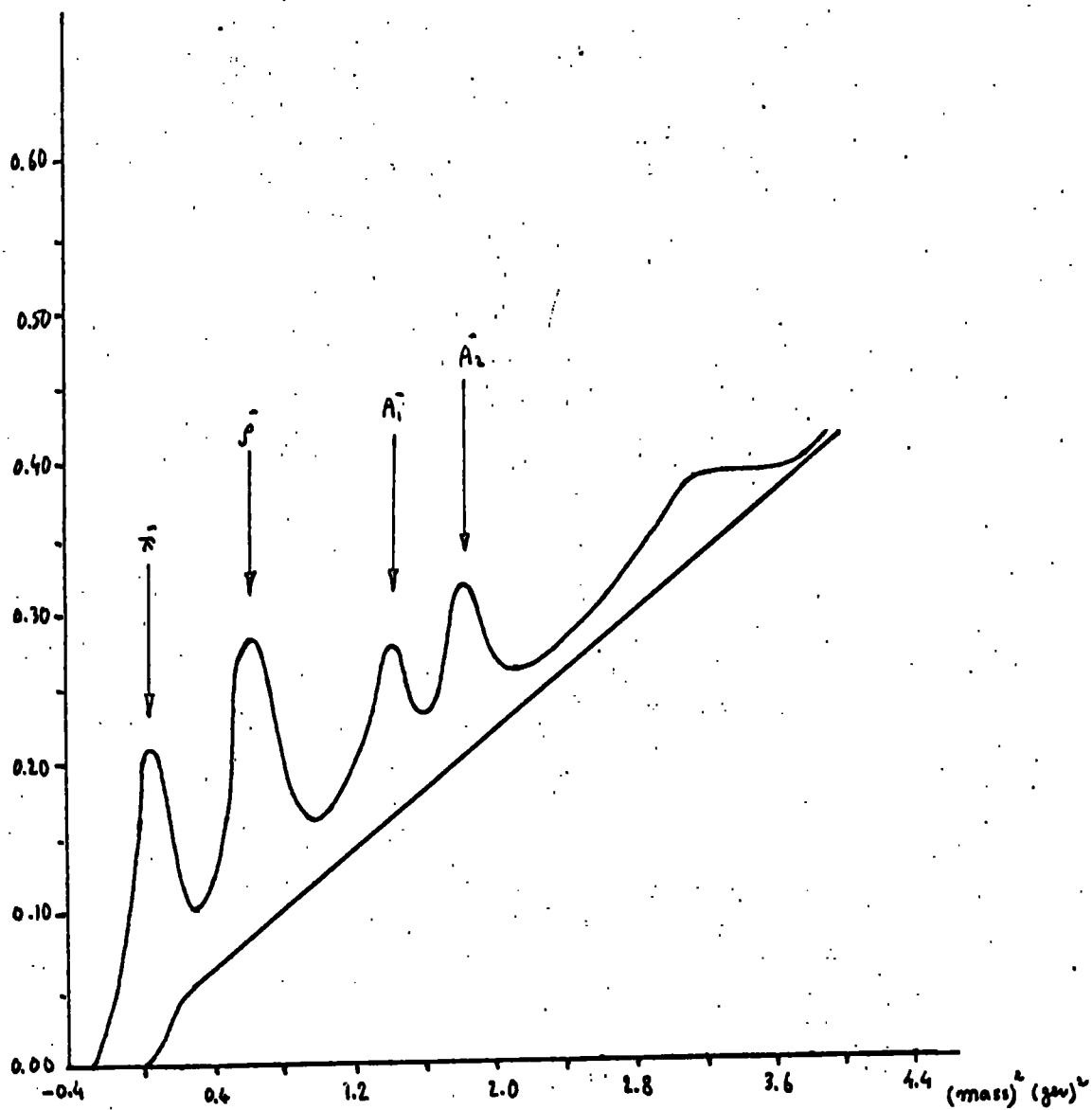


Fig 25

Fig 26

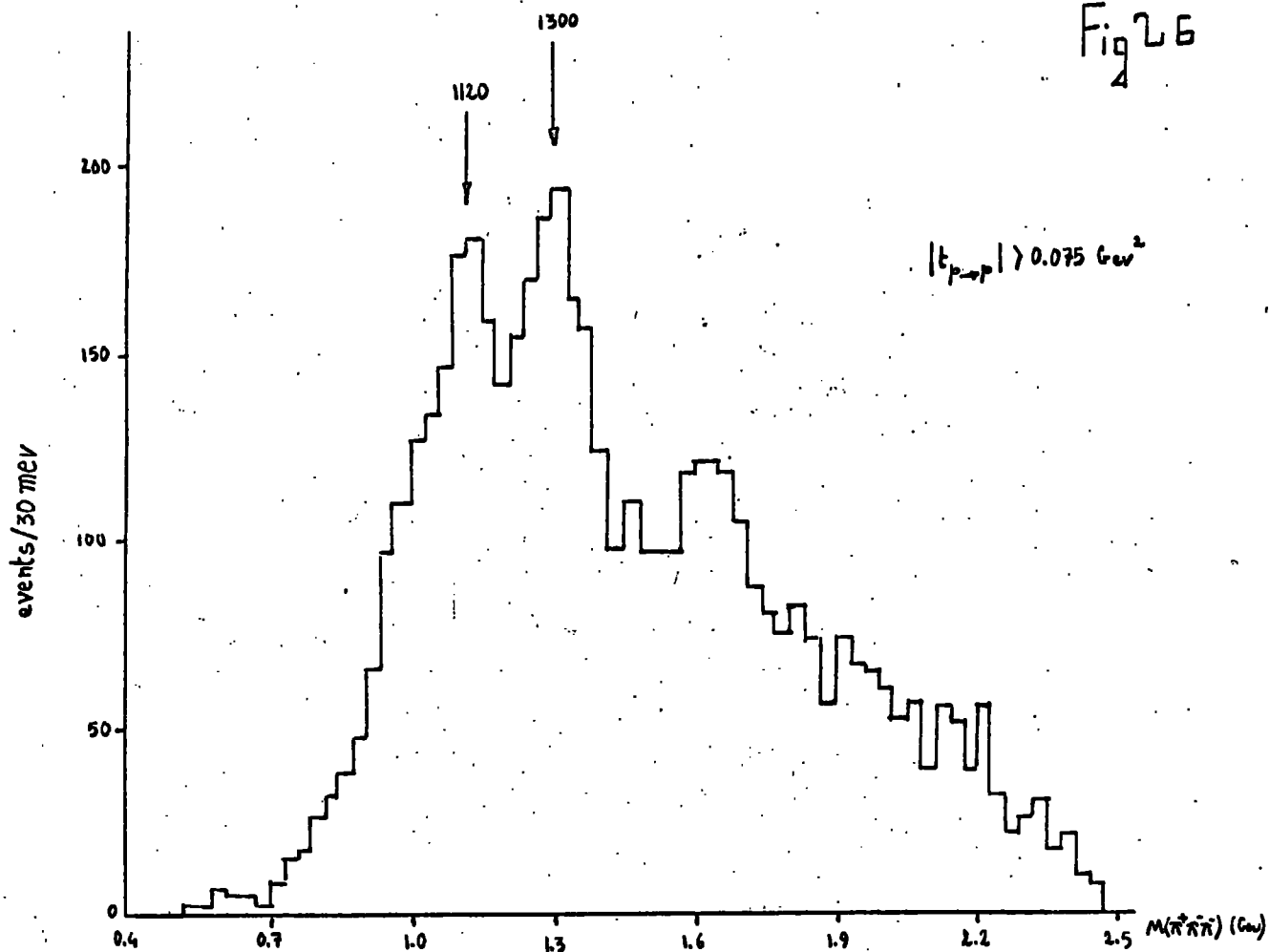


Fig 27

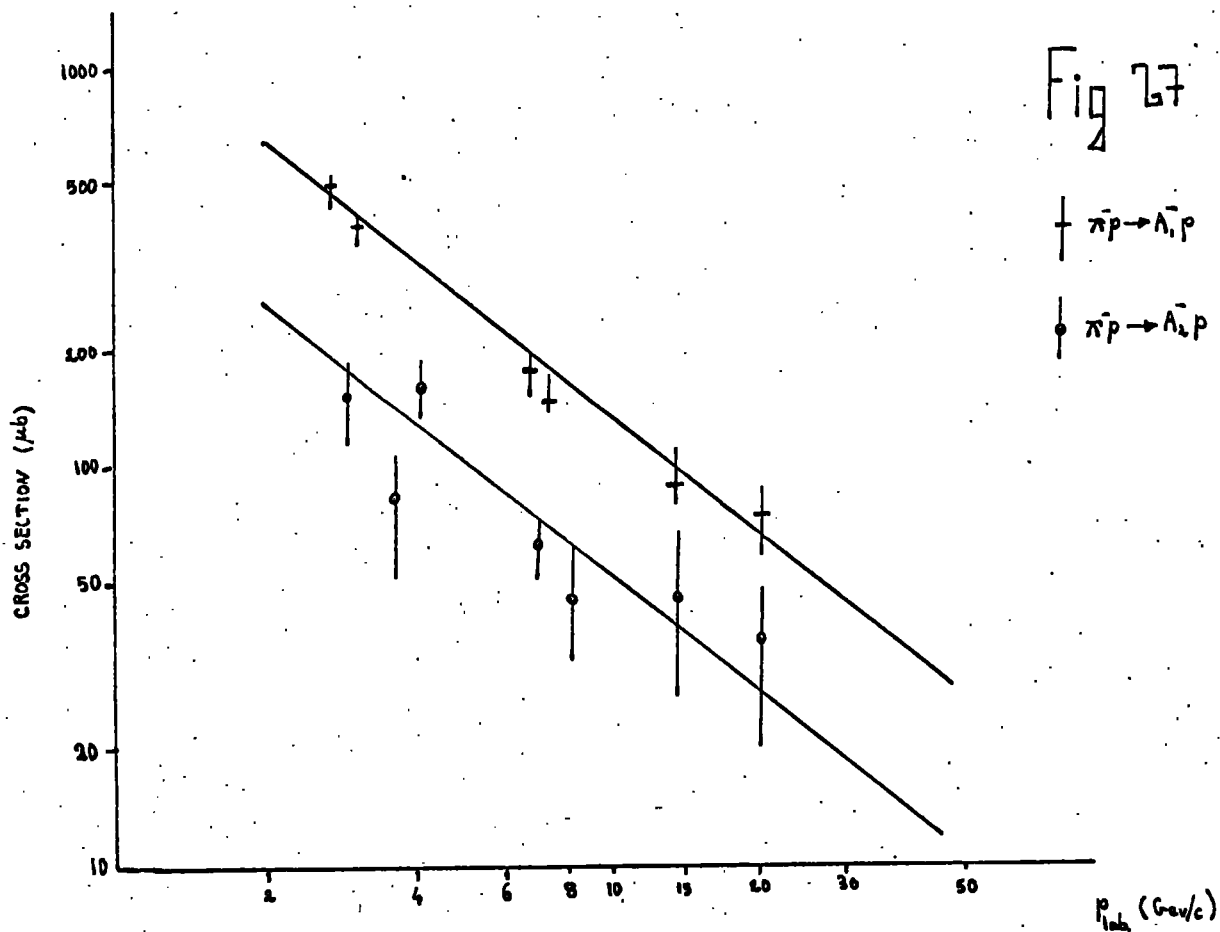
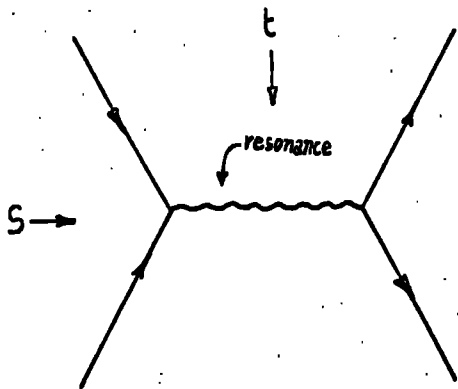


Fig 28

(a)



(b)

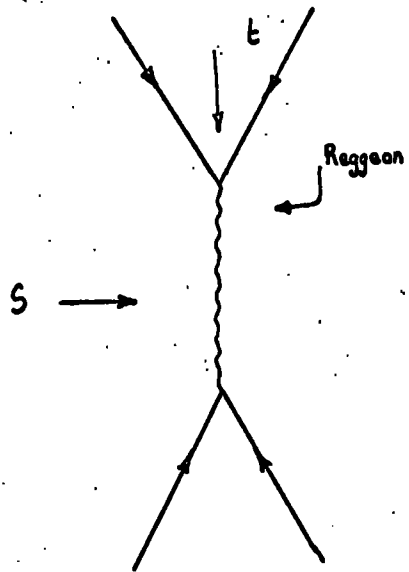


Fig 29

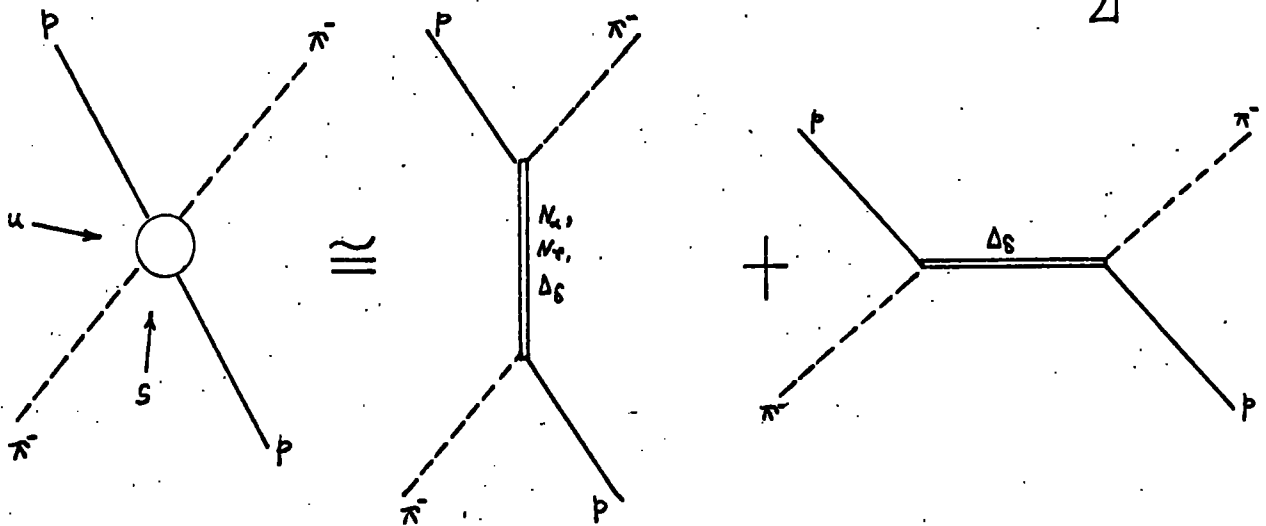
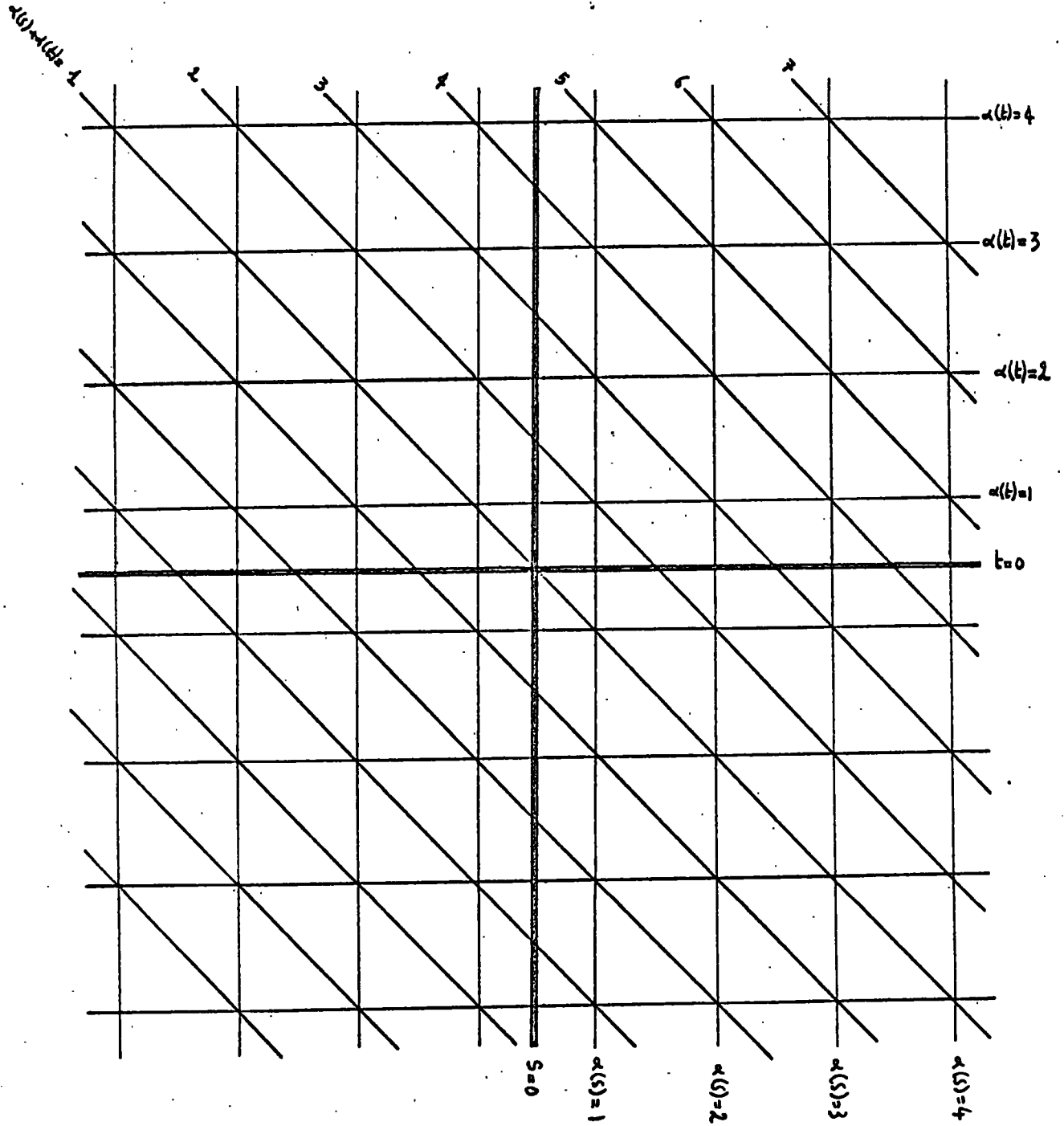
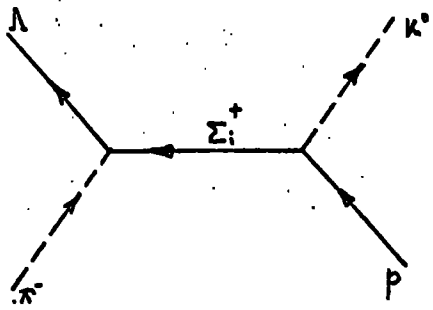


Fig 30



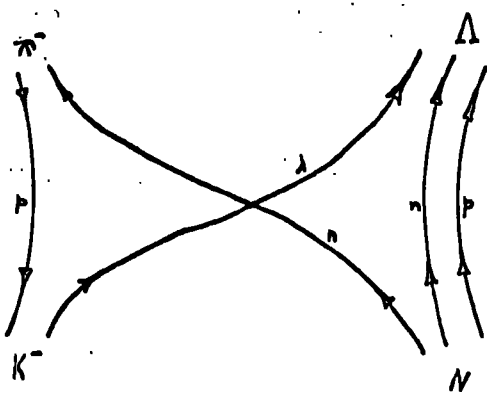
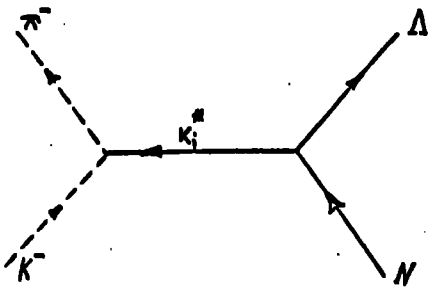


(a)

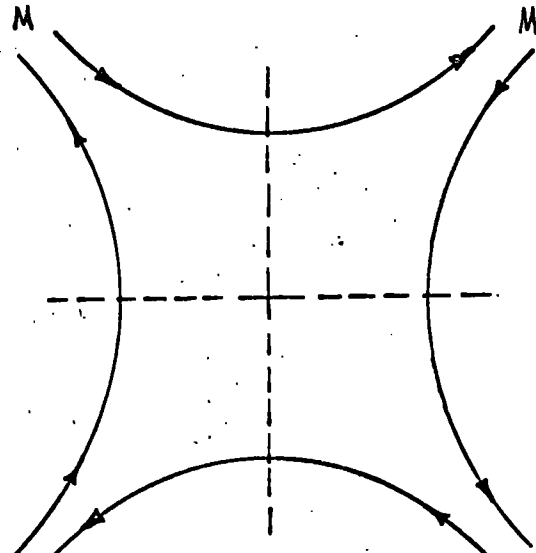
(a)

Fig 3 1

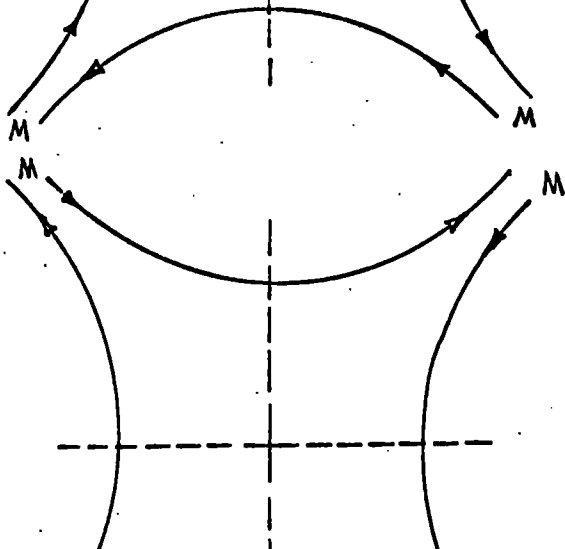
(b)



(a)



(b)



(c)

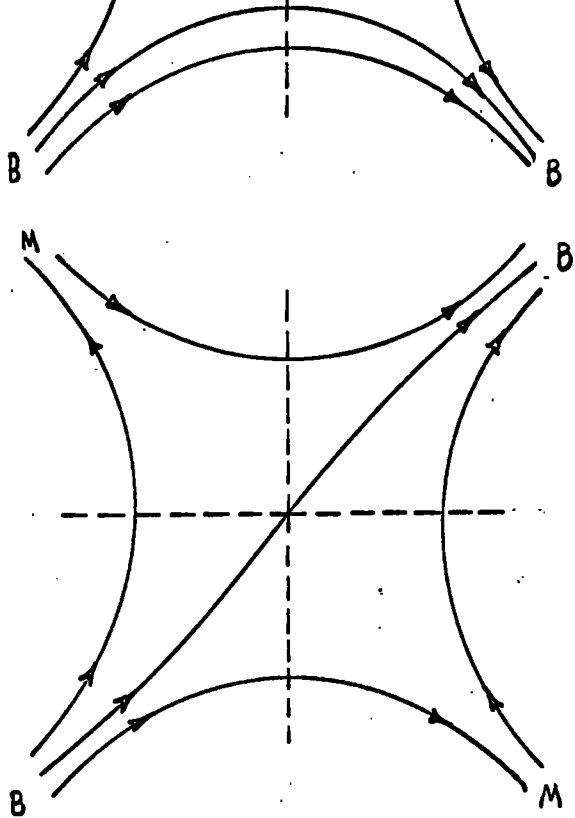
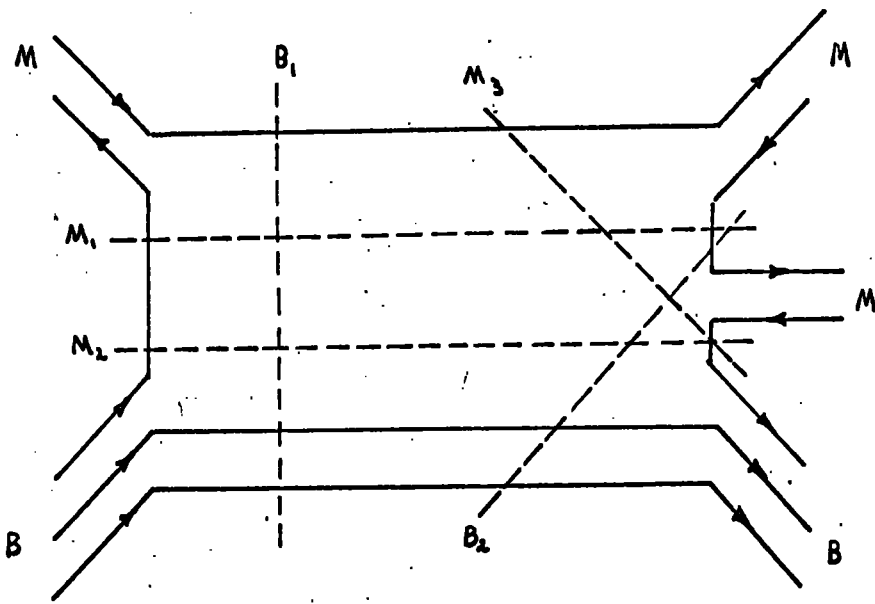
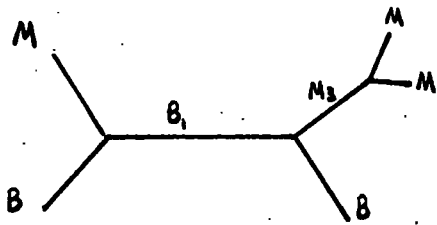


Fig 32

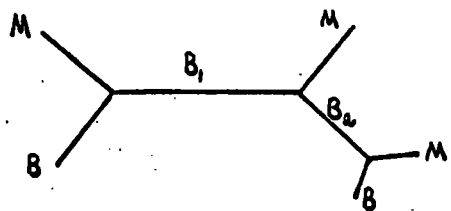
Fig 33



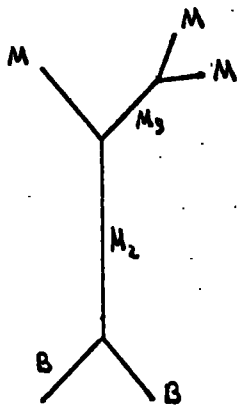
(a)



(b)



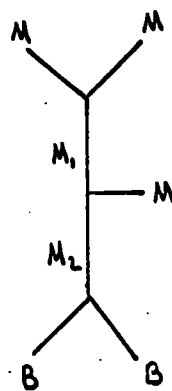
(c)



(d)



(e)



(f)

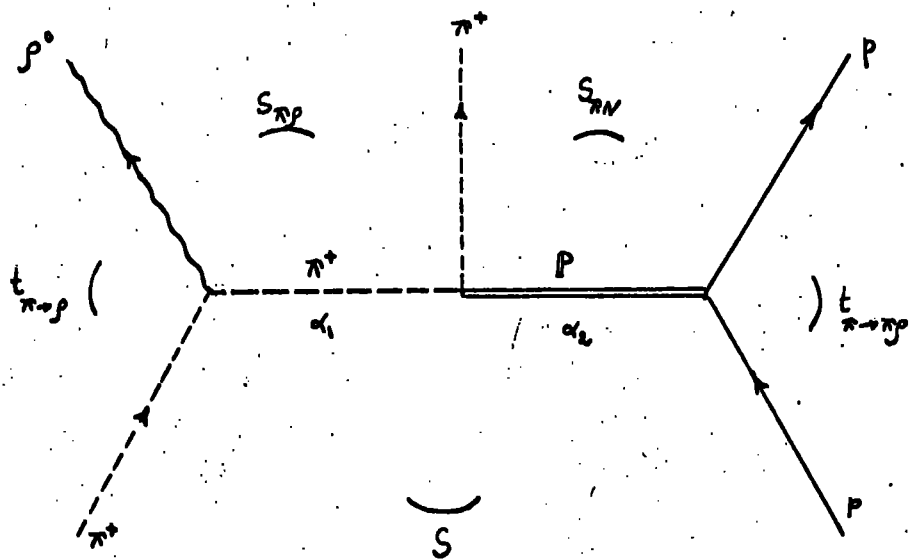


Fig 34

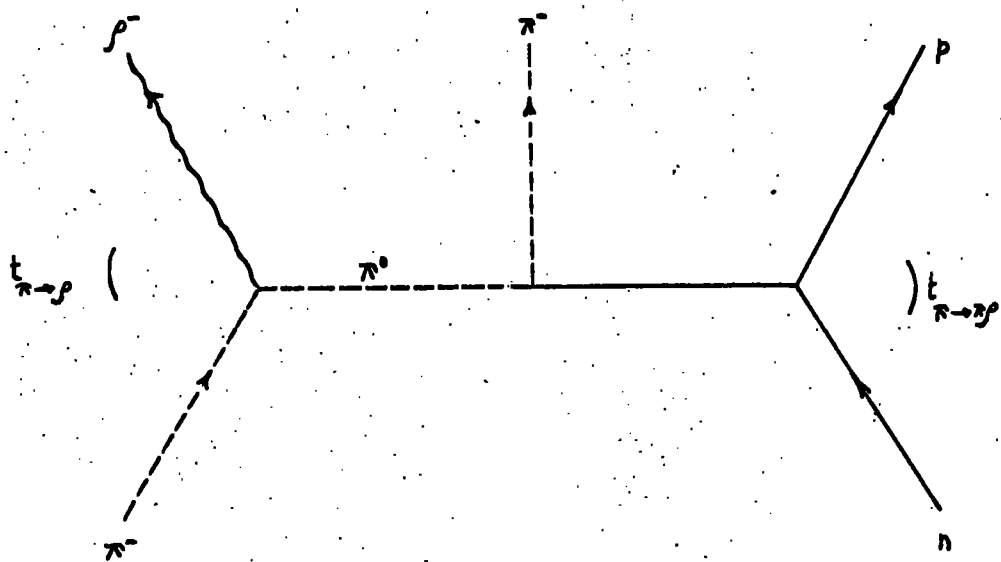


Fig 35

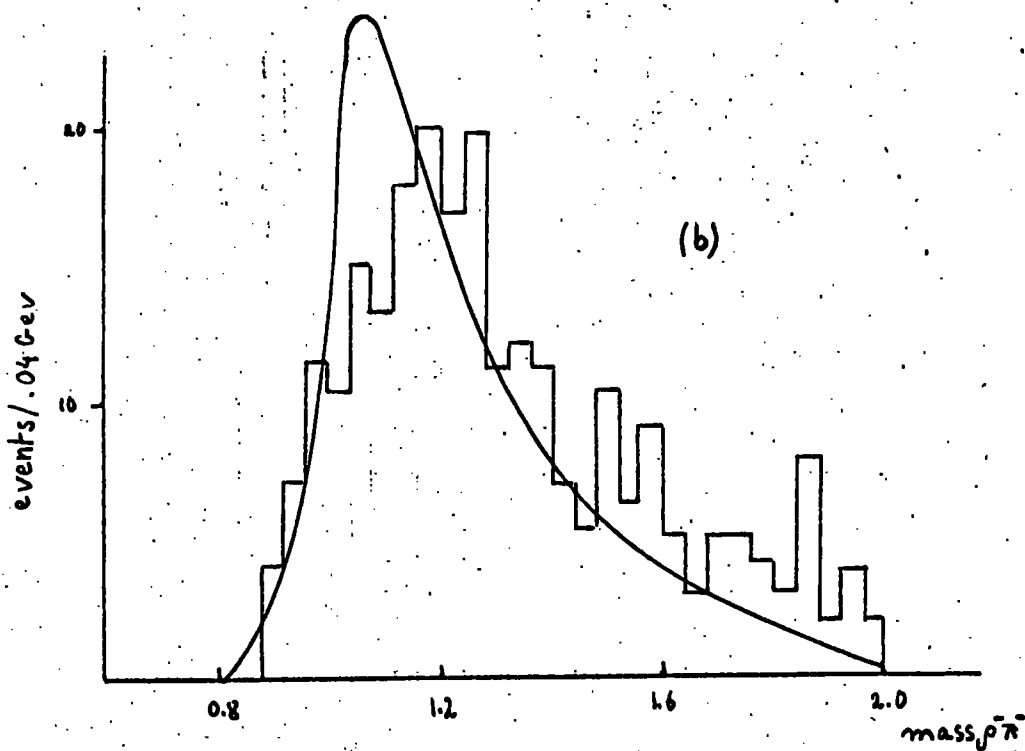
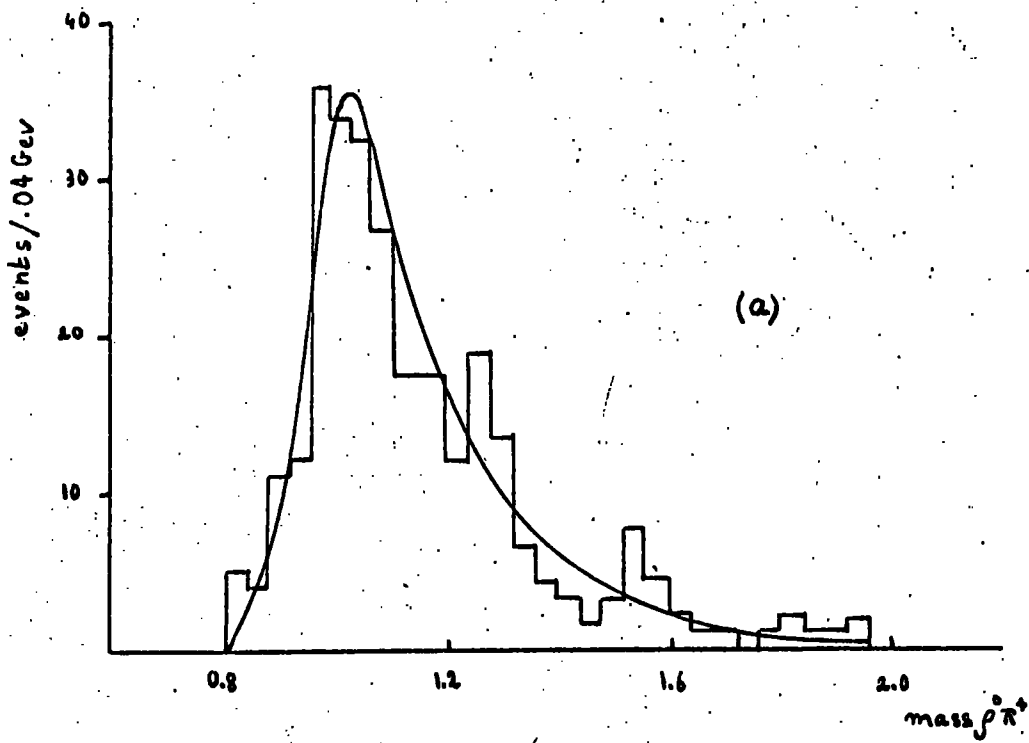


Fig 36

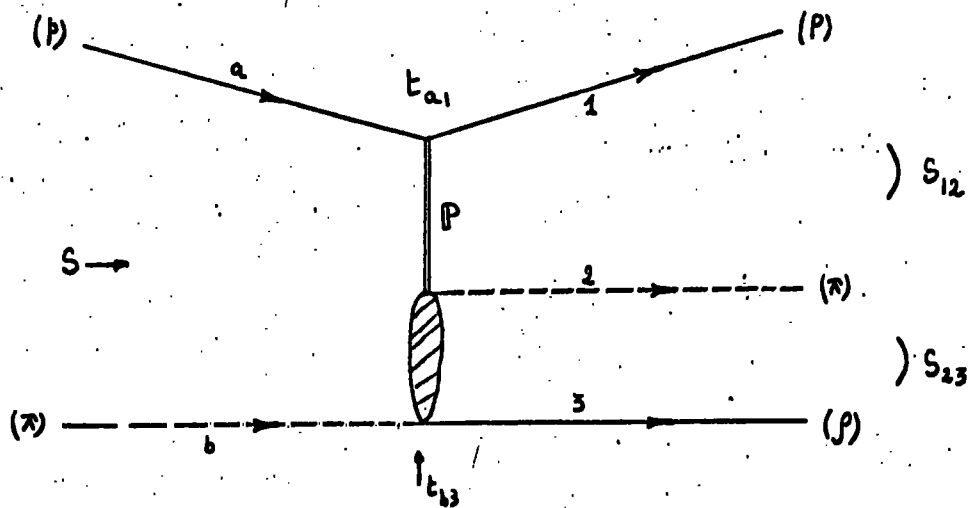


Fig 37

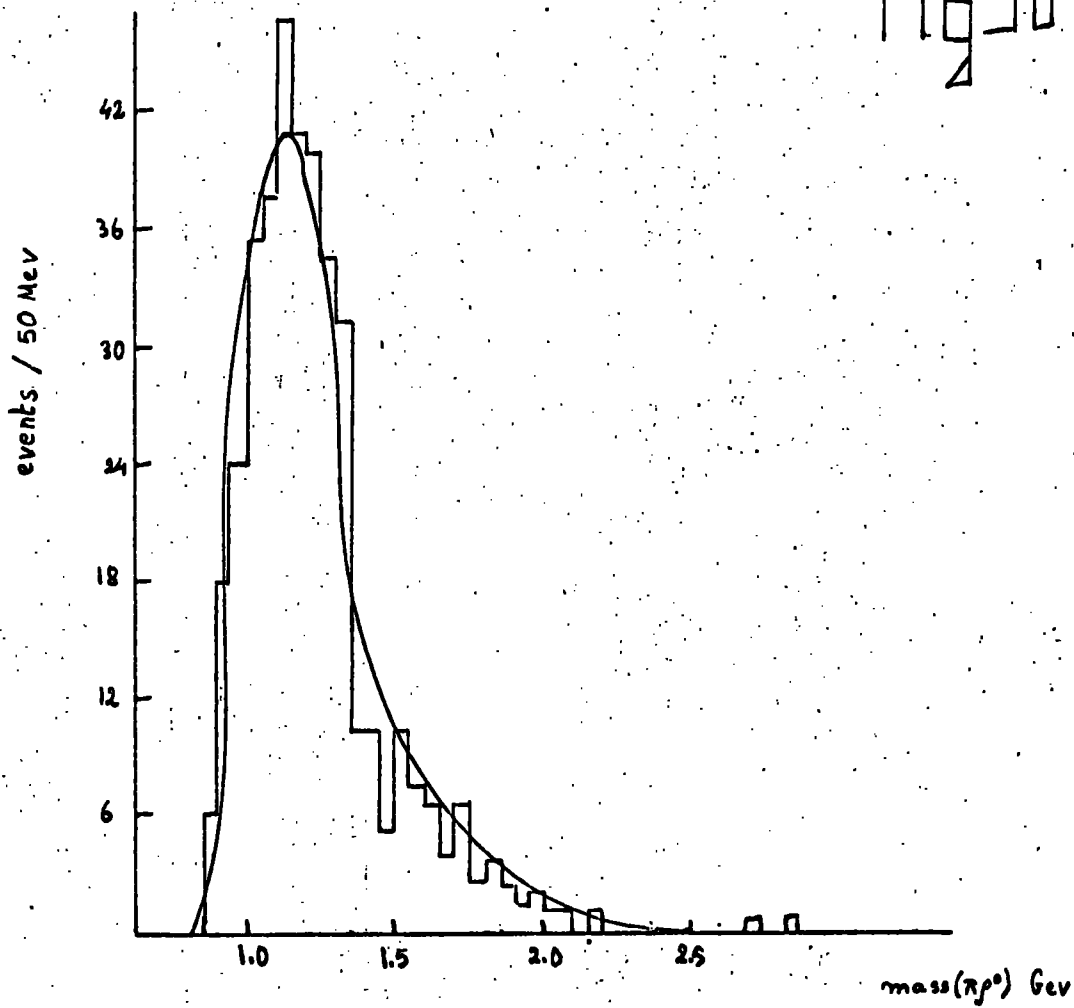


Fig 38

